Microfluidic and Organ-on-a-chip-based Technologies for Diabetes Therapy and Research

Lisa Morisseau, Taha Messelmani, Amal Essaouiba, Yasuyuki Sakai, Anne Le Goff, Cécile Legallais, Eric Leclerc, Rachid Jellali

Microfluidic and organ-on-chip based technologies for diabetes therapy and research

Lisa Morisseau [1,2≠], Taha Messelmani [1≠], Amal Essaouiba [1,2≠], Yasuyuki Sakai [2,3], Anne Le Goff [1], Cécile Legallais [1], Eric Leclerc [1,2*], Rachid Jellali [1*]

[1] *Université de technologie de Compiègne, CNRS, Biomechanics and Bioengineering, Centre de recherche Royallieu CS 60319, 60203 Compiègne Cedex*

[2] *CNRS UMI 2820; Laboratory for Integrated Micro Mechatronic Systems, Institute of Industrial Science, University of Tokyo; 4-6-1 Komaba; Meguro-ku; Tokyo, 153-8505, Japan*

[3] *Department of Chemical Engineering, Faculty of Engineering, University of Tokyo, 7-3-1 Hongo, Bunkyo-ku, Tokyo, Japan*

≠ Authors with equal contribution

* **Corresponding author:** Dr Rachid Jellali (rachid.jellali@utc.fr), Dr Eric Leclerc (eric.leclerc@utc.fr)

Abstract

Diabetes is a severe and complex disease with high prevalence worldwide. In the last few years, scientists have worked hard to understand the physiopathology of the disease, develop new treatments and diagnosis tools, and improve the quality of life of diabetic patients. Recently, there has been increased focus on using microfluidic technologies in biomedical applications, especially in diabetes research. In this chapter, we present an overview of the main microfluidic technologies related to diabetes research and how they can help solve several of the issues associated with this disease. We start by introducing diabetes, its characteristics, and its treatments. We continue with microfluidic concepts and the materials and manufacturing methods used to develop the microdevices. The main section of the chapter is dedicated to applications of microfluidic technologies in diabetes research, including sensors and diagnosis tools, pancreatic cell encapsulation for transplantation and the organ-on-chip

approach. Finally, we conclude the chapter with the perspectives for potential future developments in microfluidic technologies for diabetes and metabolic syndrome research.

1. Introduction to diabetes mellitus (DM)

The islets of Langerhans represent approximately 2% of the total pancreas and play a key role in maintaining glucose homeostasis within a narrow physiological range [1]. Blood glucose levels are controlled by two antagonistic hormones secreted by pancreatic α- and β-cells (Figure 1). In fasting periods with low plasma glucose levels, α-cells secrete glucagon to stimulate hepatic glycogenolysis and gluconeogenesis, thereby increasing blood glucose levels. Insulin secretion from β-cells is stimulated when glucose levels are elevated. Insulin release activates the uptake and storage of glucose in the muscle, fatty tissue, and liver through glycogenesis, thus lowering blood glucose levels [2,3]. Disrupted insulin secretion and/or insulin-target organ interaction leads to permanent hyperglycaemia (high levels of blood glucose) and diabetes (Figure 1) [2].

Diabetes mellitus (DM) is the most significant dysfunction of the pancreas. According to the World Health Organization (WHO) definition, DM is a chronic disease occurring when the pancreas does not produce enough insulin, or none at all, or when the body cannot use the insulin secreted [4,5]. In the most recent report (Diabetes Atlas 2019), published by the International Diabetes Foundation (IDF), it was estimated that approximately 463 million people (1 in 11 adults) have diabetes worldwide and, worryingly, that 578 and 700 million will be affected by 2030 and 2045, respectively [6,7]. Diabetes is now one of the largest global health concerns. In 2019, the IDF estimated that 4.2 million deaths among adults (20–79 years) can be attributed to diabetes [6,8]. The WHO ranked diabetes among the top ten causes of death in 2019 [5]. Diabetes is also associated with multiple complications, such as blindness, kidney failure, cardiovascular disease, sexual dysfunction, neuropathy, lower limb amputations and peripheral vascular disease [9–11]. The annual healthcare cost of diabetes was estimated at approximately 760 billion USD in 2019 and is predicted to reach 845 billion USD by 2045 [6,11].

DM can be classified into four categories: type 1 DM (T1DM), type 2 DM (T2DM), gestational diabetes mellitus (GDM), and a fourth category which includes specific types of diabetes due

to other causes such as genetic mutations, diseases of the exocrine pancreas and drug exposure [12]. T1DM and T2DM alone account for 90% to 95% of all diagnosed cases worldwide [13].

Figure 1 here

1.1. Type 1 diabetes mellitus (T1DM)

T1DM is an autoimmune disorder in which insulin-secreting pancreatic β-cells are destroyed, usually by autoimmune inflammatory mechanisms, resulting in a lack of insulin production [3,4]. This autoimmunity is due to a combination of genetic susceptibility and a host of environmental triggers such as diet, viruses, stress, and exogenous toxins [11]. The incidence of T1DM is increasing worldwide and is estimated to account for up to 10 % of diabetic patients, mostly children and young adults [13]. In addition to high blood sugar, T1DM patients present the classic symptomatology including polyurea, polydipsia, fatigue, loss of weight and blurred vision [6].

T1DM is an incurable disease. Currently, the most effective treatment is the daily administration of exogenous insulin [11]. Conventionally, insulin is administered in subcutaneous injections (with syringes) several times per day [3,13]. The blood glucose level is constantly monitored using a glucometer to help adjust the doses of insulin. Insulin can be also administered *via* an insulin pump which provides constant control of the insulinaemia, mimicking the glucose concentration patterns provided by a healthy pancreas [13,14]. Among other strategies for T1DM treatments, whole pancreas and islet of Langerhans transplants are an effective solution for restoring normoglycaemia [3,14]. However, due to the shortage of donors, the reduced number of viable extracted islets, and the need for continuous immunosuppression, the use of these strategies remains insignificant compared to the total diabetic population [3,11,13,14].

1.2. Type 2 diabetes mellitus (T2DM)

T2DM, the most common form of diabetes, comprises approximately 90% of total diabetic patients (415 million people worldwide), particularly adults aged 20-79 years [6]. It is named the

disease of the century, because its prevalence has increased exponentially in recent decades. T2DM is a complex pathology caused by insulin resistance and impaired insulin secretion [15]. Insulin resistance is characterised by the incapacity of insulin-sensitive organs (mainly the liver, muscles and adipose tissue) to uptake and properly metabolize glucose caused by impaired insulin action[11,15]. In the history of T2DM, plasma insulin level usually augments in response to insulin resistance as the result of a rise in insulin production and β-cell mass. Increase of insulin production is crucial for compensating the hormone demand caused by insulin resistance. T2DM ensues when the pancreatic β-cell fails to produce insulin at sufficient quantity for lowering blood glucose levels (loss of β-cell mass, severe β-cell dysfunction) [13,15,16]. Several factors play a role in increasing the risk of developing T2DM: genetic factors, age, obesity, unhealthy lifestyles and lack of physical activity [11,15]. The treatment of T2DM involves lifestyle modifications and antidiabetic drug therapy including orally-delivered medicines such as metformin, sulfonylureas, glinides, gliptines, glitazones and SGLT2 inhibitors, and glucagon-like peptide-1 (GLP-1) receptor agonists. Insulin injection is used when drug therapy fails to control glycemia [15].

1.3. Gestational diabetes mellitus (GDM)

GDM is defined by impaired glucose tolerance that is discovered for the first time during pregnancy. It is generally diagnosed in the second or third trimester of pregnancy [17,18]. According to the most recent IDF Diabetes Atlas (2019), 14.4% of pregnant women develop GDM (approximately 17 million births affected worldwide annually) [6]. In most cases of GDM, the glucose intolerance is related to insulin resistance and β-cell dysfunction [18,19]. The gestational diabetes risk factors include obesity, advanced age, excessive gestational weight gain, ethnicity, history of previous GDM, and a family history of TD2M [19]. The treatment of GDM consists of lifestyle adjustments and the pathology usually resolves once the pregnancy ends [4]. However, GDM is associated with several adverse outcomes, such as pregnancy complications, and an increased risk of developing T2DM and cardiovascular disease for both mother and child [18].

1.4. Other specific types of diabetes

In addition to common T1DM/T2DM and GDM, there are several other rare forms of diabetes with other causes. These forms of diabetes are caused by genetic defects in β-cell function or insulin action (monogenic diabetes), diseases of the exocrine pancreas (cystic fibrosis-related diabetes), endocrinopathies, drugs and chemicals, infection (congenital rubella, cytomegalovirus) and uncommon autoimmune forms (different from those implicated in T1DM, such as latent autoimmune diabetes in adults, LADA) [6,17,20]. Of the rare forms of diabetes, monogenic diabetes (neonatal diabetes and maturity onset diabetes of the young, MODY) is the most common, representing approximately 2% of total diabetes cases [6,20].

2. Microfluidic technology

Microfluidics refers to the manipulation and study of small-scale volumes (between microlitres and femtolitres), using devices composed of micro-structures with dimensions in the tens to hundreds of micrometre range [21]. Microfluidic technology makes it possible to miniaturise conventional laboratories in a micro-scale version with the same functionality [22]. Thanks to miniaturisation, the increase in the surface-to-volume ratio, and the continuous mode of operation, microfluidic devices have many advantages: reduced time and cost of the experiments, rapid analysis, precise control, optimisation of interactions, and enhanced functionality and reliability [21,23–25]. Furthermore, microdevices can be easily tuned by incorporating sensors, detectors, valves, pumps and electronics [24,25].

Microfluidic technology has grown exponentially and made considerable progress in the last 20 years. Nowadays, it covers a wide range of fields in the chemical, pharmaceutical, healthcare and food industries. Depending on the application and/or functionality, microfluidic devices can be called microreactors (chemistry), lab-on-chip (analysis, diagnosis) or organ-on-chip (cell, tissue and organoid culture) [26].

2.1. Materials for microfluidic devices

In microfluidics, the choice of material is fundamental and depends on the application. Several parameters regarding material properties must be considered: ease of fabrication, physical and chemical properties, chemical inertness, transparency, biocompatibility, and gas permeability [27–29]. Since the emergence of microfluidic technology, the materials used to construct microdevices have been varied and can be classified into three groups: inorganic, organic, and hybrid/composite materials [24,30]. Inorganic materials, especially silicon and glass, were among the earliest materials used in microfluidics as they are widely used in micro-electro-mechanical systems (MEMS) [31]. Silicon and glass have several suitable characteristics, such as stability at high temperatures, excellent resistance to solvents and pressure, and good surface stability [25,30]. Both materials have been used to manufacture microdevices in several fields, particularly for applications requiring the use of high temperatures and pressure, and aggressive solvents [24,26,32,33]. Nevertheless, silicon and glass present some limitations including high costs, manufacturing and bonding difficulties, and no permeability to gas (unsuitable for biological/medical applications) [26,33].

Polymers (organic materials) have played an important role in microfabrication and prototyping in the last 15 years [32]. Polymers have many advantages for manufacturing microfluidic devices as they are inexpensive, easy to access, and suitable for mass production processes. They also offer a large choice of physical, chemical and surface properties through adaptable formulations and easy chemical modifications [24,26,32]. The commonly used polymers in microfluidic device fabrication are polydimethylsiloxane (PDMS), poly(methyl methacrylate) (PMMA), cyclic olefin copolymer (COC), polycarbonate (PC), polystyrene (PS), thermoset polyester (TPE), poly(vinyl chloride) (PVC), polyurethane (PU) and polytetrafluoroethylene (PTFE) [24,26,30,32–34]. Paper, a natural, cellulose-based and biodegradable material, is also a promising low-cost substrate for microfluidics, especially in point-of-care (POC) diagnosis device manufacturing [35]. Among organic materials, PDMS is the most frequently used in microfluidic devices for biological and biomedical applications due to its key properties: high gas permeability (suitable for long-term cell cultures), biocompatibility, and good transparency

[30]. However, several disadvantages are associated with using PDMS: non-specific adsorption of molecules, absorption of less hydrophobic molecules and incompatibility with many solvents [32]. The elastomer perfluoropolyether (PFPE, fluorinated polymer) appears to be an excellent alternative to PDMS in biological applications, because of its gas permeability and chemical inertness [36–38].

In recent years, microfluidic devices from hybrid materials have been developed to improve device functionality and overcome the limitations of certain materials [24,26,30]. This approach consists in combining several materials to develop more advanced microdevices such as PDMS-glass, PDMS-PC and PDMS-NOA81 (Norland Optical Adhesive 81) devices [39–42].

2.2. Fabrication techniques for microfluidics devices

Depending on the material used, a variety of microfabrication methods are available to create the patterns in microfluidic devices such as etching, micromilling, blasting, laser ablation, optical and soft lithography, stereolithography, hot embossing, and injection molding [26,43,44]. To manufacture microstructures in silicon and glass substrates, etching is the most commonly used technique [26,45]. In this process, the undesirable material is removed using corrosive liquid chemicals (e.g., hydrofluoric acid, wet etching) or gases (e.g., octafluorocyclobutane C_4F_8 or carbon tetrafluoride CF_4, dry etching) [46]. Several other techniques can be used to pattern silicon and glass: substrate erosion by powder blasting, micromilling and laser drilling [45,46]. There are several methods for sealing glass and silicon microfluidic devices, including thermal compression, anodic and adhesive bonding [45].

For polymer-based microdevices, the microfabrication process depends on the polymer type: elastomer or thermoplastic. PDMS elastomer, the most common microfluidic substrate, is mainly micro-structured by means of simple soft lithography, a low-cost, easy-to-use process that produces high-resolution replicas (Figure 2) [26,44]. In soft lithography, the desired patterns are first fabricated on molds (master) which serve as the pattern transfer agent for the PDMS. Then, the PDMS pre-polymer is poured on to the master and heat-cured to replicate the shape. The patterned PDMS layers can easily be irreversibly sealed to each other or to glass with

plasma treatment [26,47]. Polymer photoresists (e.g., epoxy SU-8) are usually used to produce the mold using the photolithography process (Figure 2) [31,48]. Photolithography can also be used for the direct manufacture of microfluidic devices from photosensitive materials such as SU8 and thiolene polymers [24,29].

Various processes have been used to manufacture microfluidic devices with thermoplastic polymers (PMMA, PC, PS, COC, PFA), including hot embossing, injection molding, micromilling, and laser ablation. The most commonly used methods are injection molding and hot embossing, which are adapted for mass production [43,44]. Hot embossing involves pressing the mold into a thermoplastic sheet (using a hydraulic press) at a temperature higher than the softening temperature for the plastic (Figure 2). The resulting thermoplastic microdevice is the exact mirror of the mold. In the injection molding process, thermoplastic pellets are introduced into the mold's heated cavity under pressure. The microfluidic device with the desired patterns is obtained after cooling the mold (Figure 2) [26,48].

Figure 2 here

3. Microfluidic lab-on-chip for analysis and diagnosis in diabetes

Lab-on-Chip (LoC) are micro-engineered devices with integrated biosensors minted to replace conventional laboratory tests with their integrated, automated, and parallelised biochemical assays. The aim of those miniaturised platforms is to provide high sensitivity, simplicity of use, and instant results with a cost-effective scheme [49–51]. Since the publication of the first biosensor concept in 1962, consisting of an oxygen electrode for glucose measurement, glucose sensors have become the point-of-care devices (PoC) the most studied and used worldwide [52]. Biosensors can be defined as analytical devices with a biocatalyst capable of detecting a biological signal coupled to a transducer that converts the signal produced during the interaction of the biocatalyst and the analyte into a detectable parameter (Figure 3) [53].

The bio-analyte can come from a wide range of molecules, such as RNA, DNA, enzymes, metabolites, and oligonucleotides. These analytes will interact with specifically-designed biorecognition elements consisting of enzymes, antibodies, aptamers, nucleic acids, or cells.

It is noteworthy that aptamers belong to the new generation of bioreceptors composed of artificial single-stranded DNA or RNA ligands that can bind to amino acids, proteins, or large molecules. These synthetic macromolecules have high affinity and specificity thanks to the stable secondary structure that can be functionalised to attain a stronger binding force [54–56].

On the other hand, the transducer part of the biosensor can be categorised as optical, piezoelectric, calorimetric, electrochemical, acoustic, etc, and the bioreceptors immobilized on various substrates such as electrodes, nanowire arrays, transistors, or nanoparticles (Figure 3). Then, the signal is converted to digital, amplified and processed before being displayed [55].

Thanks to integration of analytical tools, LoC platforms have become the most important field of application for microfluidics, providing a sophisticated approach for sample preparation, separation, and detection [50].

LoCs are trending PoC diagnosis devices due to their versatility, reliability, simplicity, cost-effectiveness, and portability. In recent years, microfluidics have played a crucial role in the development of PoC devices for chronic diseases, with numerous approaches covering both diagnosis and management applications [57]. Currently, the gold standard in diabetes detection and aetiopathogenic group classification is quantification of glucose and insulin levels in blood samples [58]. Unfortunately, these two parameters are not considered specific biomarkers for early detection of DM [59–61]. This is particularly true of measuring blood insulin levels, as the test is often carried out when the patient already presents symptoms typical of the disease [62,63]. However, studies have shown that markers such as C-peptide (a byproduct of insulin production), glycosylated haemoglobin (HbA1c), glycated human serum albumin (HSA), C - reactive protein (CRP), and adiponectin are key indicators for early DM detection [57,64,65].

Figure 3 here

3.1 Microfluidic-based methods for DM diagnosis

3.1.1 Paper-based analytical device (μPAD) for glucose measurement

To tackle one of the major drawbacks of current glucose measurement methods, paper-based analytical devices (μPAD) have shown great potential for rapid and low-cost detection. Their

compatibility with commercial printing technology and good limit of detection (LOD) ranges make them a fast diagnostic tool for glucose detection and monitoring [58,66]. The main advantage of µPADs compared to glucose meter test strips is their ability to confine a small amount of sample thanks to the hydrophobic barrier in a hydrophilic cellulose-based device. This drastically improves the efficiency and control of reagents, making it possible to parallelise and measure multiple analytes at the same time [57].

Many original approaches have been reported in the last decade to increase accuracy or reduce the assay time and amount of sample (Table 1) [67–70]. For example, Evans et *al*. developed a filter paper-based µPAD functionalised with silica nanoparticles with the purpose of enhancing the colour homogeneity of colorimetric glucose detection. Their device uses a small size sample (10 µL) and the assay time is around 30 min [71]. Meanwhile, Shechi et *al*., reported a shorter assay time (20 min) and an even smaller size sample (3 µL) but they did not mention the LOD of their 3D µPAD device [72]. Palazzo et *al*., used gold nanoparticles to functionalise the µPAD with the aim of avoiding the colour bleaching that usually happens with these enzyme-based devices [73]. Another approach, proposed by Kugumiya et *al*., combines spectrometric measurement of hydrogen peroxide resulting from the enzymatic reaction in the microfluidic chip [74]. A recent breakthrough microfluidic chip was reported by Zhang et *al*., where the detection method in the colorimetric assay was performed with a smartphone application instead of the conventional scanner. They also used an innovative inkjet printing method for the fabrication, to enhance the performance of the µPAD, obtaining an LOD of 0.01 mg/ml and reducing the assay time to only 5 min [75].

µPADs are definitely recognised as a breakthrough analytical platform for multiple biosensing applications as pointed out by Nadar et *al*., in a recent review, where they provide an extensive insight into design, fabrication, and enzyme immobilisation strategies for developing enzyme-µPADs [76]. However, despite their excellent qualities, such as the high speed and low-cost production processes, µPADs still have some practical issues to overcome. These are mainly the fragility of the material and the difficulty separating the hydrophilic regions from the hydrophobic ones [77,78].

3.1.2 Lab-on-chip based devices for glucose & immune marker detection

With the aim of revealing a reliable indicator for diabetes, an accurate and precise indicator is glycated haemoglobin (HbA1c). HbA1c levels are the ratio of glycated haemoglobin and total haemoglobin in the bloodstream, which reflects the average blood glucose level for the preceding 2-3 months [5,64,79]. Usually, HbA1c measurement is carried out with immunoassays, high-performance liquid chromatography (HPLC), or mass spectrometry (MS). However, these methods are time-consuming and not cost-effective. The limitations related to the high cost and handling complexity of MS have been overcome thanks to the development of small, low cost, and simple operating LoC with integrated mass spectrometers which have the potential to make MS more accessible to clinical laboratories (Table 1) [57]. For instance, Mao et *al.,* reported a silicon nanoLC-MS microfluidic device to determine healthy patients from T2DM patients using only 5 µL of blood sample. The platform makes it possible to quantify glucose, HbA1c, glycated HSA, and glycated apolipoprotein A1 (apoA-1) within the same microfluidic device [64]. In another study, Redman et *al.,* developed a capillary electrophoresis-mass spectrometry (CE-MS) device to indirectly measure HbA1c through glycated β-Hb and HAS, also in a blood sample. Capillary electrophoresis simplifies the sample mixture and improves the resolution of the signal intensity [80]. Independently, Li et *al.,* developed a unique aptamer-based microfluidic system for automatic HbA1c and Hb simultaneous measurement via magnetic beads. The high performance of their technology relies on reducing reagent consumption by 75% and time of analysis from 3h30 to 30 min when compared with traditional HPLC [81]. Similarly, Chang et *al.,* used an aptamer-based microfluidic system to detect HbA1c and Hb with high sensitivity and specificity even for a smaller sample (50 µL) in relatively shorter time (25 min) [82].

In addition to HbA1c measurement for DM diagnosis, it was imperative to develop PoC systems for the ethiopatogenic group classification. Therefore, Zhang et *al*., proposed a plasmonic gold chip for the detection of autoantibodies against several pancreatic islet antigens (insulin, glutamic acid decarboxylase (GAD65) and tyrosine phosphatase islet antigen 2 (IA2)). The plasmonic gold platform enabled simultaneous detection and quantification of

autoantibodies to islet antigens and their isotypes with an exceptionally high specificity and sensitivity that cannot be reached by classic ELISA assay using only 2 µL sample [83].

3.1.3 Red blood cells (RBC) deformability test

Researchers have discovered that, in addition to the molecular biomarkers, DM detection can be also carried out analysing the stability and deformability of erythrocytes or red blood cells (RBC) (Table 1). For example, Zhan et *al.,* proposed a microfluidic platform to study RBC fragility based on the characterisation of osmotic lysis kinetics from the point of view of fluid mechanics [84]. The lysis kinetics were traced by measuring the release of intracellular contents using a CDD camera coupled with a microscope. The change in erythrocyte fragility after exposure to glucose was detected using this LoC at high sensitivity by recording the light intensity of the RBC at several locations in the microchannel [84]. Cha et *al*., proposed a tool for measuring cell stretching based on the focusing of three-dimensional viscoelastic particles, with high accuracy. Moreover, the authors used the platform to monitor the decrease in deformability due to nutrient starvation in human mesenchymal stem cells [85]. In another different approach, Tsai et *al.,* developed a new method based only on stiffness of the "equilibrium velocity" of erythrocytes in a microchannel. The value of this approach lies in the elimination of viscosity, which is a time-dependent feature making it possible to evaluate cell stiffness alone [86]. An extensive review by Bento et al. compared the different approaches proposed in the literature to characterise RBC deformability in a microfluidic device [87].

3.2 LoC-based methods for DM management

In DM, the continuous monitoring of blood glucose, insulin, c-peptide, and other markers at home is crucial for disease management. For this reason, telemedicine and the progress made in miniaturised cyber technology is revolutionising PoC devices for diabetes management (Table 1). Accordingly, Yao et *al.,* developed a PDMS microfluidic-based telemedicine system for real-time insulin detection. The method for monitoring insulin is based on sandwich immunoassay combined with luminal-hydrogen peroxide (H_2O_2) chemiluminescence. With a

photometer, the microfluidic device detects the peak value of the luminous intensity, which indicates the insulin concentration in the patient's blood sample [65]. Nowadays, enzyme electrode sensors are not widely used for continuous glucose monitoring in clinics because of their short lifetime, interference with the body's bioelectricity, and, most importantly, their invasiveness [57]. For instance, Yang et al. developed a multiple enzyme-doped thread-based microfluidic system with a polyvinylchloride (PVC) coated membrane for rapid and low-cost electrophoresis separation and electrochemical detection of glucose in whole human blood [78]. Meanwhile, Pu et al. reported a different microfluidic chip with an integrated sensor based on an electrochemical electrode functionalized with graphene and gold nanoparticles (AuNPs) [88]. The purpose of the coating combination on the working electrode was to enhance the resolution of glucose sensitivity. This sensor could measure glucose precisely in the linear range from 0 to 162 mg/dl with an LOD of 1.44 mg/dl; this novel approach has the potential for tackling the current clinical challenge of continuous glucose monitoring for hypoglycaemia diagnosis [88]. In return, Yin et *al.,* reported an optical fiber sensor integrated microfluidic chip for ultrasensitive glucose detection using long-period grating inscribed in a small-diameter single-mode fiber as an optical refractive-index sensor. Their experimental results have shown that such a powerful device has not only an ultralow detection limit (1 nM), but also a remarkably fast response time (70 s) [89].

Table 1 here

4. Microfluidic biochips for islet or β-cell encapsulation

Transplanting islets of Langerhans or β-cells is an attractive alternative to exogenous insulin in the treatment of T1DM as it maintains coherent and sustained control of glucose homeostasis. However, the need for permanent immunosuppression limits its application [3,90]. The encapsulation of islets/β-cells within a selectively permeable membrane is an increasingly prevalent method for protecting cells from immune rejection. This concept, called the bioartificial pancreas (BAP), provides efficient immune-isolation, while allowing the exchange of oxygen, insulin, hormones, and nutrients through the membrane [91,92]. Depending on the

dimensions of the BAP device, the encapsulation process can be classified in two categories: micro- (device size 250-1000 µm) and macroencapsulation (device larger than 1 mm) [91].

The microencapsulation process is particularly interesting as it generates microcapsules with a high surface-to-volume ratio, making possible a high diffusion capacity and easy implantation procedures. However, there are several limitations due to the methods (extrusion, dripping and emulsification) used to generate microcapsules, including high polydispersity, large microcapsules (generally close to 1 mm) and poor repeatability [93,94]. The size of the BAP plays a key role in the functionality and survival of the transplanted cells. Large microcapsules lead to limited exchange of oxygen, nutrients and insulin between the host and BAP (the distance between encapsulated cells and vasculature must not exceed 150-200 µm) [95,96]. The limited oxygen and nutrient supply causes hypoxia and apoptosis, and reduces insulin secretion, resulting in failure of the transplant.

Microfluidic technology offers several advantages for cell encapsulation, with a variety of biocompatible polymers such as polysaccharides, proteins, and polyethylene glycol (PEG). Microfluidic devices can produce uniform microcapsules in sub-100 micron diameters, with thin membranes and very low variation coefficients (< 3%) [93,94]. The capsules' diameter and membrane thickness can easily be tuned by varying the dimensions and geometry of the channels, plus the flow rate and viscosity of the polymer solution [97]. Furthermore, microfluidic-based encapsulation offers the capacity for high-throughput production with high reproducibility. In recent years, several studies reporting cell (including insulin-secreting cell) encapsulation using microfluidic technology have been published [94,95,98–103] (Figure 4A, 4B). Tomei et *al.,* reported conformal coating of islets with PEG and PEG-alginate using a microfluidic flow-focusing method. This method minimises capsule size and thickness, which improves oxygen, and insulin exchange and graft volume. Transplanting microcapsules into the renal subcapsular space in mice makes it possible to maintain euglycaemia for 102 days [95]. Microfluidic devices were also used for hiPSC-derived pancreatic cell high-throughput encapsulation within alginate/chitosan. The process makes it possible to generate uniform

microcapsules (70 µm in diameter) containing islet organoids with high expression of α- and β-cell markers and responsive to glucose challenges [103].

Although small microcapsules enhance diffusion, viability, and cell functionalities, they are difficult to trace, replace, and retain within the implantation site. Another approach for developing a BAP consists of encapsulating the islets or β-cells in microfibers. The use of microfibers with a low diameter offers the advantage of working with devices that are easy to handle, while good diffusion properties are preserved [104,105]. Of the methods used in microfiber engineering, microfluidic technology offers several advantages compared to conventional processes (such as electrospinning and extrusion): high reproducibility, easy customisation of the dimensions and morphological features, and adaptability for cell encapsulation and *in vivo* immunoprotection [106]. A variety of microfluidic designs have been used to encapsulate islets, β-cells and other mammalian cells using different polymer matrices (Figure 4C, 4D) [105,107–112]. Using a microfluidic co-axial device (Figure 4C), the Takeuchi group developed microfibers encapsulating extracellular matrix (ECM) proteins and islets or β-cell lines within alginate and alginate/ polyacrylamide matrices. The microfibers formed were transplanted into diabetic mice and were able to secrete insulin and normalise blood glucose concentrations for a period of up to 100 days [105,111,113]. In another approach, to overcome the problem of pancreatic cell shortages, Jun et *al.,* encapsulated hybrid spheroids (hepatocytes/pancreatic cells) into alginate/collagen microfibers using a cylindrical flow channel in a PDMS-based microfluidic chip (Figure 4D). They observed effective control of glucose levels by the hybrid microfibres transplanted into the diabetic mice [109].

Figure 4 here

5. The pancreas organ-on-chip model

Organ-on-chip (OoC) is defined by Bathia and Ingber as a microfluidic device dedicated to living cell cultures. Cells are continuously perfused within micro-chambers in order to reproduce the behaviours of *in vivo* tissues and organs [114]. Thanks to progress in microfabrication, biomaterials and cell engineering, OoC technology has become a powerful

tool for reproducing physiological cell behaviour *in vitro* and replacing the traditional paradigms based on animal experiments and 2D *in vitro* cell culture methods [114–116]. Of the others, OoC technology makes it possible to construct a well-controlled microenvironment and create "physiological-like" situations such as zonation, cell-cell interaction, shear stress, and chemical gradients [114].

Although OoC technology generates a suitable microenvironment that reproduces endocrine function, there is less development of the technology for the pancreas than for other tissues or organs, such as the liver, lung, kidney, gut, and heart [11,117]. Pancreas-on-chip applications for diabetes research can be classified in three groups: islet evaluation, drug research, and the study of islet physiology and function [118].

To mimic the *in vivo* physiology and functionality of native islets as much as possible, pancreas-on-chip models are developed using cultures of islets, or cells aggregated into spheroids (pseudo-islets). The pseudo-islet approach makes it possible to engineer uniform, small-sized spheroids (< 150 µm), which enhance oxygen and nutrient diffusion, viability and functionality when compared to native islets (heterogenous size 50-400 µm) [119,120]. Pseudo-islets can be engineered by aggregating β-cells, iPSC-derived β-cells or primary β-cells obtained after islet dissociation [121]. To maintain the islets/pseudo-islets under flow inside the microfluidic biochip, trapping microstructures fabricated in the microchambers of the device are used (Figure 5). Micro-wells with different geometries (flat, pyramidal and concave) are the most commonly used designs for islet trapping [119,122–129]. Islets can also be immobilised using crescent-shaped structures [130], mesh systems [131], nozzle systems, or channel reduction, [132–134] and other constructions involving hydrodynamic trapping principles [117,135].

Figure 5 here

5.1 Potential cell sources for pancreas-on-chip models

The success and capacity of *in vitro* pancreatic models to reproduce *in vivo* physiology and functionality depend on the cell types used and their sources [11]. The potential cell sources for

in vitro models can be classified in four groups: human primary islets of Langerhans or β-cells, animal primary islets of Langerhans or β-cells, cell lines (human or animal: EndoC-βH, MIN6, INS-1,RIN5-F and αTC1.9) and induced pluripotent stem cells (iPSCs) [11,121,136–142]. The advantages and limitations of the different cell types are summarised in Figure 6.

Primary human β-cells or islets isolated from cadaveric organs are still considered to be the gold standard for transplantation and *in vitro* pancreatic models [121]. Due to their origin, they accurately reflect the physiology and functionality of the organ *in vivo*. However, the shortage of donors, the high costs associated with isolating islets, and the high variability limit their application [136,143]. For animal primary cells, although they are widely used because of their attractivity (availability and stability), there are considerable limitations, including functional differences between animal and human islets, inter-species variability and ethical concerns [121,143]. As an alternative to primary islets, several animal (MIN6, INS-1, RIN5-F and αTC1.9) and human (EndoC-βH1-3) β-cell lines have been investigated [137–140]. Nevertheless, they present several lacunae, such as limited functionality, and differences in the expression of β-cell markers when compared to primary cells [143,144].

In recent years, β-cells derived from stem cells have emerged as an attractive source of pancreatic cells. Stem cells have the ability to self-renew and differentiate into most of the body's cell types, including pancreatic cells [143]. The use of embryonic stem cells (ESCs) raises ethical problems and is strictly regulated (prohibited in some countries) [145]. hiPSCs do not raise any ethical problems and offer the possibility of developing patient-specific models with the genetic background associated with the disease desired [136,143]. The differentiation of hiPSCs into pancreatic β-cells has been widely reported in the literature [141,142,146–148]. However, the high cost and inability of obtaining fully mature β-cells remain an obstacle to the generalisation of use of hiPSCs [143].

Figure 6 here

5.2 Pancreas-on-chip for islets physiology study

Circumstantial evidence has shown the existence of fluctuations in plasma glucose and insulin levels [149]. Under *in vivo* conditions, islets are subjected to a dynamic environment in which insulin is secreted by β-cells in a biphasic pattern. Pyruvate oxidation by the tricarboxylic acid cycle (TCA) in mitochondria is the signalling pathway involved in insulin release. In brief, glucose catabolism generates ATP through TCA, which leads to an increase in the intracellular ATP/ADP ratio and closure of ATP-sensitive potassium (KATP) channels. As a result, the plasma membrane depolarises and the Ca^{2+} voltage-dependent channels (VDCCs) open. The rapid influx of glucose-stimulated Ca^{2+} triggers fusion of insulin granules with the cell membrane and subsequent exocytosis of insulin, C-peptide, and proinsulin. Thus, rapid stimulation of β-cells with glucose induces biphasic insulin secretion with a first phase corresponding to a rapid increase in the rate of secretion for 4-8 min. This is followed by a decrease in the insulin rate and a second stable or gradually increasing phase which lasts as long as the glucose simulation is applied [150]. Impairment of dynamic insulin release can have a severe influence on glucose homeostasis and related physiological functions. Loss in the first phase, reduction in the second phase, and impairment of the oscillatory pattern of insulin secretion are, for example, characteristic features of T2DM and contribute significantly to its progression. Therefore, studying dynamic insulin secretion is crucial for understanding the pathogenesis and pathophysiology of diabetes, as well as for assessing pharmacokinetics and potential action mechanisms of anti-diabetic medication [151].

In the past decade, many research groups have specialised in developing microfluidic perfusion system (MPS) for islet physiology research (Table 2) [152–156]. Currently, integrating analytical throughput into microfluidic devices is of great interest for studying the pulsatility of pancreatic hormone secretion by detecting and monitoring the electrical, biochemical, and ionic signalling activities of β-cells. As an example, Xing et *al.* developed pumpless microfluidic devices including real-time fluorescent imaging and insulin secretion kinetics for both mouse and human islets [157]. Their results showed an increase in intracellular calcium and a typical biphasic profile of insulin secretion, affirming the involvement of calcium oscillations in the

phenomenon of pulsatile insulin secretion. In fact, coherent insulin and calcium oscillations are either disturbed or lost in patients with T2DM [158]. To standardise the pancreatic islet model, Misun et *al.* designed a hanging drop microfluidic chip that showed significant potential for enhancing the spatiotemporal resolutions of stimuli, and sampling and observing molecular signals. Reaggregated islets produced physiologically close and reproducible insulin secretion with a pronounced first phase and pulsatile second phase throughout, indicating robust cellular communication and synchronisation [151]. Other studies have reported a dissociation between oscillations of insulin secretion and glucose, suggesting that other metabolic signals may be involved. However, their efficacy has been demonstrated to be less than that dependent on Ca^{2+} concentration oscillations [159,160]. In another strategy, Patel et *al.* developed an organoid microphysiological platform combining dynamic 3D cultures, optical assessment, and functional assays, while also limiting the quantity of sample required [161]. Replacing standard culture dishes with their MPS platform made possible an *in situ*, temporal, and live cell assessment of the dynamic impact of glucolipotoxicity on pancreatic islets. Outcomes revealed an increase in Ca^{2+} signalling and a rate of dead cells in the β-cells exposed to high glucose-fatty acid media when compared to β-cells exposed to basal glucose media. These findings are consistent with the theory that hyperlipidaemia and hyperglycaemia contribute to the impaired β-cell function observed in T2DM [162]. Microfluidic biochips are thus a promising tool for studying the mechanisms and restoration of insulin secretion in diabetic islets.

5.3 Pancreas-on-chip for islets evaluation and preservation

Microfluidic biochips have been explored extensively to assess the functionality of pancreatic islets (Table 2). For instance, the pressure and flow volume of the islet vascular system can be reproduced, making these platforms ideal for *in vitro* islet analysis. This technology could thus make it possible to reduce bioartificial pancreas failure by obtaining precise knowledge of the quality of a donor's pancreatic tissue and accelerating studies in drug discovery and toxicology.

Prior to transplantation, islets are checked through rigorous quality control to assess their viability, morphology, hormone secretion, and response to glucose-stimulation. The *in vitro* gold standard for evaluating islet quality is static 2D culture using conventional Petri dishes or multi-well plates. Although this model has significantly contributed to medical research, it presents certain limitations. To determine how the culture conditions affect gene expression in islets, Jun et *al.,* compared expression levels of islet-specific genes in islet spheroids cultured in microfluidic biochips under static or dynamic conditions and islets cultured in Petri dishes using conventional methods for 7 and 14 days [119]. The results showed that β-cell genes such as insulin, Pdx1, and Glut2 had significantly higher expression in dynamic groups than in intact or static groups. They demonstrated that a microfluidic platform makes long-term islet maintenance possible for up to 1 month. Essaouiba et *al.,* developed a microfluidic biochip composed of 600 micro-wells for assessment of rat islets and showed that biochip culture improves the viability and expression of pancreatic genes [126]. In a different strategy, islets were cocultured with mesenchymal stem cells (MSCs) to investigate the viability and preservation of islet functions. MSCs have been shown to secrete several paracrine molecules, which mediate trophic effects on neighbouring cells [163,164]. Lin et *al.,* used a coculture microfluidic chip where rat bone marrow mesenchymal stem cells (BM-MSCs) and islets were introduced respectively into 2 microchambers which could be connected by a traffic tunnel [165]. They reported that the BM-MSCs had the ability to migrate to the microchamber containing murine islets and provide improved GSIS during 3 to 21 days of culture.

In vivo pancreatic islets are heavily vascularised with fenestrated endothelial cells (ECs) to facilitate blood glucose sensing and endocrine hormone secretion. The close proximity of insulin secreting β-cells and ECs plays a major role in modulating the proliferation and survival of both cell types [166]. Transplanting isolated islets causes disruption in their vascular connections, making the islets dependent on the formation of new blood vessels for optimal function. Evidence from experimental islet transplants indicates insufficient revascularisation of transplanted islets with subsequent chronically decreased blood perfusion and oxygen tension, which has metabolic consequences within the tissue [167]. It has effectively been

established that during *ex vivo* culture, the characteristic cobblestone morphology of ECs is deteriorated, leading to a rapid decline in cell density (-50% in the first day and total loss after 7 days of culture) [168]. The Rocheleau research group postulated that this deterioration occurs in the absence of blood flow due to limited diffusion of media inside the tissue. Thus, they developed a haemodynamic environment using a custom-designed microfluidic device to test the effect of fluid flow on the maintenance of rat islet ECs [132]. Outcomes revealed that isolated pancreatic islets treated with media flow in a microfluidic device achieved wide-reaching diffusion within the tissue of serum albumin, which is an anti-apoptotic signal for ECs [169]. Although they observed a significant reduction in necrosis in flow-treated islets, EC morphology was only partially maintained [133]. To improve previous results, they explored treatments to stimulate endogenous expression of angiogenic factors. The data suggested mild hypoxia as a potential method for slowing the demise of ECs while maintaining islet β-cell function [170].

Other perfused well platforms were developed by the Easley research group to assess the dynamics of hormone secretion from endocrine tissues. Based on their first report of mouse primary adipocyte cultures within microfluidic systems [171], they developed a robust method for a temporally-resolved examination of endocrine tissues, including pancreatic islets. The concept consists in a macro-to-micro interfacing of microfluidic systems using 3D-printed interface templates [172]. The main results highlighted that glycerol release rates from adipocytes increased after exposure to low glucose and insulin levels (LGLI). In this way, they investigated a fully automated 16-channel microfluidic input/output multiplexer composed of 3D-printed templates to interface both islets and adipose tissue [173]. This system served essentially as a mimic of the circulatory system and upstream endocrine signals, while allowing dynamic and quantitative measurements of both hormone secretion and nutrient sensing/uptake. In addition, the device provided new information on temporally-resolved free fatty acid exchange in adipose tissue.

Recently, hiPSCs-derived organoids have emerged as a new class of *in vitro* organ models for disease modelling and regenerative medicine. Tao et *al.,* presented a new strategy for creating

heterogeneous human islet organoids derived from hiPSCs using organ-on-chip technology [125]. The islet organoids generated displayed suitable tissue morphology and multicellular complexity resembling human pancreatic islets *in vivo*. Moreover, they showed enhanced expression of mature β-cell associated genes and proteins, insulin secretion levels, and Ca^{2+} flux release ability in response to glucose under perfused culture conditions, highlighting the role of biomimetic mechanical cues in enhancing islet organoid function and maturation. Therefore, human islet-on-a-chip provides a proof of concept for synergistic engineering of heterogeneous islet organoids from hiPSCs by combining organ-on-a-chip technology and stem cell development biology [130].

5.4 Pancreas-on-chip for drug development and screening

Insulin secretagogues are antidiabetic medications that aim to increase the insulin output of pancreatic islets. They include sulfonylureas such as tolbutamide, glinides and incretin-related drugs such as dipeptidyl peptidase 4 (DPP-4) inhibitors, and glucagon-like peptide-1 receptor (GLP-1R) agonists which are widely used to treat type 2 diabetes [174]. The process for studying and developing anti-diabetic drugs usually depends on *in vivo* animal models and *in vitro* 2D monolayer cell culture models. Although animal models and 2D cell cultures have made significant medical contributions, there is a lack of predictability when results are extrapolated to humans because of anatomical and physiological differences. Ramachandran et *al.,* highlighted evidence of these differences in a study where re-aggregated human pancreatic islets were assessed and compared to native human islet and rat islet drug screening [175]. The response of the different islets was significantly different when tested against a variety of compounds such as the calcium channel agonist Bay K 8644, glibenclamide, tolbutamide, caffeine, carbachol, and glucagon-like peptide-1, among others. As the authors pointed out, islet reaggregates may represent a more homogenous model for drug screening as native islets are heterogenous in terms of both size and composition.

Currently, several works are being carried out on developing *in vitro* models to improve medical prediction. Recent progress in microfabrication, cell engineering, and imaging technologies

have led organ-on-a-chip to become an innovative technology capable of reproducing physiological cell behaviours and drug screening (Table 2). For instance, in order to study compound-stimulation mechanisms for insulin secretion, Misun et *al.,* exposed reaggregated islets to tolbutamide and exendin-4, a sulfonylurea-class compound and a glucagon-like-peptide 1 receptor (GLP-1R) agonist respectively [151]. Continuous tolbutamide treatment resulted in a sharp increase of the first-phase insulin secretion, which could lead to severe hypoglycaemia if treatment timing is not respected. On the other hand, exendin-4 showed a potentiated action on glucose-induced insulin secretion by a most pronounced second-phase with sustained oscillations, which is consistent with a previous study by Ritzel et al.,[176]. Therefore, recent progress in β-cell signalling studies in biochips have not only enhanced our understanding of insulin secretion, but also revealed the mechanisms of insulin secretagogues. Immunosuppressive medication, which is an inevitable part of islet transplants, could also benefit from OoC technologies. Several studies have demonstrated that OoC devices can provide a robust platform for testing the compatibility of the immunosuppressive regimen with the immune system, as well as the effect of immunosuppressive reagents on isolated islet function and viability [118].

In physiological conditions, cells reside in a three-dimensional (3D) environment and interact with other cells and the extracellular matrix (ECM) [177]. These interactions are necessary for the proper differentiation and function of typical cells, and they more precisely mimic physiological pathological conditions. With this in mind, Jun et *al.,* performed a drug efficacy test on rat islet spheroids cultured under dynamic conditions [119]. They tested two typical antidiabetic drugs, tolbutamide and glucagon-like peptide-1 (GLP-1), at different concentrations. The results revealed that islet spheroids under dynamic conditions exhibited higher sensitivity to drugs. These outcomes were also demonstrated by Essaouiba et *al.,* on both native rat islets and hiPSC-derived islets [126,130]. Moreover, for drug toxicity testing, Jun et *al.,* exposed the islet models to rapamycin, which has been used in islet transplantation as an immunosuppressant. Higher toxicity resistance in the dynamic group reflects that *in vitro* toxicity assays may produce significantly different results depending on the culture environment [119]. For drug screening

applications, spheroid biochip models can improve assay reproducibility and quality with enhanced response to therapeutics.

Table 2 here

6. Multi-organ-on-chip for diabetes research

T2DM has been linked to different causes, particularly dysfunctions affecting β-cells, growing resistance to insulin, or chronic inflammatory conditions which cause the loss of control of blood glucose levels. It is a multi-organ disease involving interactions between different organs including the pancreas, liver, muscles, nervous system, kidneys, adipose tissue, and small intestine (Figure 7) [11]. The inter-organ specificity of T2DM is due to the endocrine and exocrine functionalities of the pancreas. The pancreas contains exocrine glands producing important enzymes for digestion, including trypsin, amylases, and lipase which break down respectively proteins, carbohydrates, and fats in the intestine. This enzyme mix is routed through the pancreatic duct and joins the bile duct to reach the duodenum in the small intestine, its site of action. On the other hand, the endocrine function of the pancreas is centred on islets of Langerhans, which are responsible for releasing important hormones into the bloodstream. The main hormones are insulin and glucagon, which act to control blood sugar. Maintaining sugar homeostasis is imperative for the functioning of the rest of organs [178].

To understand the biological processes and develop therapeutic strategies for T2DM, scientists conventionally used *in vivo* models because of the complexity and integrated multi-organ responses they confer. However, these models tended to fail due to the phylogenetic distance between humans and animals, and their use has been limited for ethical reasons [11,179]. An alternative to these models is the use of *in vitro* methods; the reference technique relies on the classic culture of primary cells using *in vitro* culture platforms. These strategies aim to investigate cells' biological responses without controlling the context surrounding them. This kind of simplification results in the model failing to mimic key aspects of the human body [180]. To obtain physiologically meaningful and reproducible data, it is important to generate models that take the different organs involved into account. Different research has focused on

this subject and tried to develop culture systems that combine different organs to reproduce T2DM. The most recent innovations used organ-on-chip technology to reproduce the behaviour of an organ or a group of organs. This technology improves the transport of nutrients, oxygen, hormones, and metabolic waste to create a “physiological-like” condition. The idea is to combine different cell types in different culture compartments (each compartment mimicking a specific microphysiological condition) and connect them through microfluidic channels to mimic and ensure the crosstalk between two or more organs [181].

Most of the time, multi-organ-on-chip tries to faithfully emulate the *in vivo* environment and interactions between organs. The implied signalling pathways create synergic effects on cells which enhance their functions compared to monocultured cells [182]. Despite the potential that these approaches offer for reproducing the multi-organ interactions implied in DM, several limitations are encountered in reference to the optimisations needed to ensure the optimal culture of the different cells, vascularisation of the organs, which has not yet been mastered, and standardisation of the materials and cells in the models used which causes variabilities that could impact results [183].

Figure 7 here

6.1 Liver pancreas-on-chip

The liver is the largest organ in the human body and has an indispensable role in overseeing digestion, metabolism, and the elimination of toxins from the body. In patients with T2DM, the liver is one of the first organs to be severely affected by insulin resistance and reacts to this by increasing the production of glucose. Many hepatic *in vitro* models and liver-on-chip have been introduced and advanced to reproduce hepatic functions and architecture [11]. Only a few studies have focused on the pancreas and its interactions with the liver to produce a liver-pancreas multi-organ-on-chip [184]. Recent works have demonstrated the potential for OoC technology to ensure pancreatic islet-liver crosstalk. Bauer et *al.,* designed a two-organ-chip system to ensure the dynamic culture of human pancreatic islets and liver spheroids composed of the HepaRG cell line and primary human stellate cells [178] (Figure 8A). The aim of their study was

to develop a reliable human T2DM model. They observed an increase and a conservation of insulin secretion which supported stabilisation of the homeostatic state when comparing the co-culture condition with the monoculture. In addition, they confirmed that islet microtissues lose their function after being subjected to prolonged hyperglycaemia. In another approach, Essaouiba et *al.,* used a perfusion loop with two biochips hosting primary hepatocytes and rat islet to investigate the interaction between the organs compared with monoculture conditions [184] (Figure 8B). They proved that co-culturing pancreatic cells with hepatocytes helped to recover hepatic functions (compared to the hepatic monoculture without insulin) and modified the expression of the genes involved in insulin/glucagon homeostasis.

Integrating multiple organs on a chip has always been a challenging goal because of the optimisations that must be taken into consideration to allow optimal culture of all the cell types involved in the system. Lee et al. developed a pancreas-muscle-liver OoC, given the relation that links these 3 organs [185]. Indeed, *in vivo*, the muscle is responsible for the most important glucose uptake of the body. As a consequence, signalling pathways are activated in the pancreas to produce glucagon, and start glucose production in the liver (gluconeogenesis and glycogenolysis) and the clearance of insulin [186]. In addition to the experimental results obtained from glucose metabolism stimulation, the combination of the multi-organ-on-chip led to the construction of a mathematical model describing time-dependent concentration changes in glucose and insulin.

Figure 8 here

6.2 Organ-on-chip coupling pancreas and other organs

The small intestine and the pancreas crosstalk through a complex endocrine system composed of hormones. In the case of T2DM, endogenous insulin is affected, leading to its deficiency or diminished effectiveness. Nguyen et *al.,* focused on this connexion and developed an endocrine system on chip reassembling insulin-secreting β-cells and immortalised L-cell lines, which are located in the small intestines that stimulate insulin secretion when exposed to glucose intake from diet [139]. In normal conditions, the glucose intake

sets off the production of glucagon-like peptide-1 (GLP-1) by the L-cells, which in turn activate the secretion of insulin by the β-cells. The authors observed that after 3 days of culture, and after exposure to a glucose stimulus, the multi-organ-on-chip system responded by an increase in, and saturation of, the insulin level. These results were compared to 2D static cultures and monocultures of the two cell lines separately, and the OoC exhibited higher expression of insulin. The results demonstrated the potential of the endocrine system on a chip to screen GLP-1 analogues and stimulants and ensure follow up of natural insulin production in the treatment of diabetes [139].

The pancreas interacts also with adipose tissues. Several studies have proved the supportive effects, anti-inflammatory role, and immunomodulatory properties of these tissues on the viability, structure, and insulin production of β-cells. This has been studied by Lu et *al.,* who developed a co-culture system composed of 3 cell chambers, two holding adipocytes connected to one holding islets [187]. Then to study the interactions between the two cell types, the adipocyte perfusate, containing adipocyte secretions, passes into the islets chamber. GSIS was measured in different conditions to analyse the co-culture effect. They observed an increase of insulin production in the co-culture condition compared to monocultured one. These results highlight the endocrine interaction between adipocytes and islets by delivering cytokines and growth factors, which promotes cellular functions [188].

Although multi-organ-on-chip technology provides a powerful tool for recapitulating several “physiological” situations and studying organ-to-organ crosstalk, further developments are needed to accurately mimic *in vivo* native tissues. The construction of 3D tissue onto the biochip represents a promising approach for reproducing the behaviour of an organ or a group of organs and providing a more appropriate micro-environment for tissue maintenance and development [189]. While pancreas-on-chip models usually use 3D cultures of islets of Langerhans or β-cells spheroids, cells are still mostly cultivated in 2D (monolayer inside the biochip) for the majority of other OoC such as liver, muscle and adipose-on-chip. Recent advances in tissue engineering, biomaterials, and microfabrication technology offered the opportunity to create OoC with complex 3D tissues combining multiple cell types [181,190]. Several

approaches can be used for 3D cell culture: design of hydrogels and scaffolds, cell aggregation in spheroids, 3D bioprinting, and 3D printing of microfluidic biochip [190-193]. In recent years, many 3D organ-on-chip models have been reported in the literature including liver- [194-198], muscle- [199-201] and adipose-on-chip [202,203]. These models have been shown to produce the key characteristics and functionalities of *in vivo* tissues/organs. The combination of such models with pancreas-on-chip to build multi-organ-on-chip devices can reproduce accurately the physiological interactions between pancreas and organs related to DM, and help to elucidate the pathophysiological mechanisms in diabetes.

7 Conclusions

In this chapter, we have presented the basic concept of microfluidic technologies linked to diabetes. More particularly, we have shown how microfluidics can be used as one of the essential building blocks for various bioengineered solutions in the fight against metabolic syndrome and related disorders, with a focus on diabetes. Of these solutions, the point of care approach can take part in enhancing patient autonomy by providing technologies that can be carried out easily in daily life. Regarding the disease model, the organ-on-chip solution makes it possible to access human models involving complex crosstalk and organ-to-organ interactions. Organ-on-chip coupled with the adequate cell sources, obtained from patient-derived iPSCs, will in a near future contribute to reproducing human variability and the idiosyncrasy encountered in heterogenous patient populations. Overall, we believe that microfluidics will play a part in generating advanced tools suitable for large-scale, personalised medicine solutions. In addition to conventional animal models, microfluidic-based technology contributes to bridging human *in vitro* models, human cohort data, and patient therapy.

List of abbreviations

2D	Two-dimensional
3D	Three-dimensional
ADP	Adenosine diphosphate
ADSCs	Adipose-derived stem cells
ATP	Adenosine triphosphate
AuNPs	Gold nanoparticles
BAP	Bioartificial pancreas
BM-MSCs	Bone marrow mesenchymal stem cells
C_4F_8	Octafluorocyclobutane
Ca^{2+}	Calcium ions
CDD	Charge-coupled device
CF_4	Carbon tetrafluoride
COC	Cyclic olefin copolymer
CRP	C -reactive protein
DM	Diabetes mellitus
DPP-4	Dipeptidyl peptidase 4
ECM	Extracellular matrix
ECs	Endothelial cells
ESCs	Embryonic stem cells
GDM	Gestational diabetes mellitus
GLP-1	Glucagon-like peptide-1
Glut2	Glucose transporter 2
GSIS	Glucose-stimulated insulin secretion
H_2O_2	Hydrogen peroxide
HbA1C	Glycosylated haemoglobin
hiPSCs	Human-induced pluripotent stem cells
HSA	Human serum albumin
IDF	International Diabetes Foundation
iPSCs	Induced pluripotent stem cells
KATP	ATP-sensitive potassium
LADA	Latent autoimmune diabetes in adults
LGIL	Low glucose and insulin levels
LOD	Limit of detection
MEMS	Micro-electro-mechanical systems
Min	Minutes

mm	Millimetre
MODY	Maturity onset diabetes of the young
MS	Mass spectrometry
MSCs	Mesenchymal stem cells
nM	Nanomolar
NOA81	Norland Optical Adhesive 81
OoC	Organ-on-chip
PC	Polycarbonate
PDMS	Polydimethylsiloxane
Pdx1	Pancreatic and duodenal homeobox 1
PEG	Polyethylene glycol
PFA	Perfluoroalkoxy alkane
PFPE	Perfluoropolyether
PMMA	Poly(methyl methacrylate
POC	Point-of-care
PS	Polystyrene
PTFE	Polytetrafluoroethylene
PU	Polyurethane
PVC	Polyvinyl chloride
RBC	Red blood cells
T1DM	Type 1 diabetes mellitus
T2DM	Type 2 diabetes mellitus
TCA	Tricarboxylic acid cycle
TPE	Thermoset polyester
USD	United States dollar
VDCCs	Voltage-dependent channels
WHO	World Health Organization
µPAD	Micro paper-based analytical device

References

1 N. Jouvet and J. L. Estall, *Exp. Cell Res.*, 2017, **360**, 19–23.

2 P. V. Röder, B. Wu, Y. Liu and W. Han, *Exp. Mol. Med.*, 2016, **48**, e219.

3 R. Jellali, A. Essaouiba, E. Leclerc and C. Legallais, in *Current Trends and Future Developments on (Bio-) Membranes*, Elsevier, 2020, pp. 77–108.

4 E. Maillard and S. Sigrist, in *Biomaterials for Organ and Tissue Regeneration*, Elsevier, 2020, pp. 299–333.

5 World Health Oorganization (WHO) Official Web Site.

6 IDF Diabetes Atlas 9th edition 2019, https://www.diabetesatlas.org/en/, (accessed 22 May 2021).

7 P. Saeedi, I. Petersohn, P. Salpea, B. Malanda, S. Karuranga, N. Unwin, S. Colagiuri, L. Guariguata, A. A. Motala, K. Ogurtsova, J. E. Shaw, D. Bright and R. Williams, *Diabetes Res. Clin. Pract.*, 2019, **157**, 107843.

8 P. Saeedi, P. Salpea, S. Karuranga, I. Petersohn, B. Malanda, E. W. Gregg, N. Unwin, S. H. Wild and R. Williams, *Diabetes Res. Clin. Pract.*, 2020, **162**, 108086.

9 K. Papatheodorou, M. Banach, E. Bekiari, M. Rizzo and M. Edmonds, *J. Diabetes Res.*, 2018, **2018**, 3086167.

10 J. L. Harding, M. E. Pavkov, D. J. Magliano, J. E. Shaw and E. W. Gregg, *Diabetologia*, 2019, **62**, 3–16.

11 J. Rogal, A. Zbinden, K. Schenke-Layland and P. Loskill, *Adv. Drug Deliv. Rev.*, 2019, **140**, 101–128.

12 Z. Punthakee, R. Goldenberg and P. Katz, *Can. J. Diabetes*, 2018, **42**, S10–S15.

13 S. Szunerits, S. Melinte, A. Barras, Q. Pagneux, A. Voronova, A. Abderrahmani and R. Boukherroub, *Chem. Soc. Rev.*, 2021, **50**, 2102–2146.

14 B. Kepsutlu, C. Nazli, T. B. Bal and S. Kizilel, *Curr. Pharm. Biotechnol.*, 2014, **15**, 590–608.

15 R. A. DeFronzo, E. Ferrannini, L. Groop, R. R. Henry, W. H. Herman, J. J. Holst, F. B. Hu, C. R. Kahn, I. Raz, G. I. Shulman, D. C. Simonson, M. A. Testa and R. Weiss, *Nat.*

Rev. Dis. Prim., 2015, **1**, 1–22.

16 D. Tripathy and A. O. Chavez, *Curr. Diab. Rep.*, 2010, **10**, 184–191.

17 A. D. Association, *Diabetes Care*, 2019, **42**, S13–S28.

18 J. F. Plows, J. L. Stanley, P. N. Baker, C. M. Reynolds and M. H. Vickers, *Int. J. Mol. Sci.*, 2018, **19**, 3342.

19 H. D. McIntyre, P. Catalano, C. Zhang, G. Desoye, E. R. Mathiesen and P. Damm, *Nat. Rev. Dis. Prim.*, 2019, **5**, 1–19.

20 A. T. Kharroubi, *World J. Diabetes*, 2015, **6**, 850.

21 G. M. Whitesides, *Nature*, 2006, **442**, 368–373.

22 M. I. Khot, M. A. Levenstein, G. N. de Boer, G. Armstrong, T. Maisey, H. S. Svavarsdottir, H. Andrew, S. L. Perry, N. Kapur and D. G. Jayne, *Sci. Rep.*, 2020, **10**, 1–13.

23 P. S. Dittrich and A. Manz, *Nat. Rev. Drug Discov.*, 2006, **5**, 210–218.

24 K. Ren, J. Zhou and H. Wu, *Acc. Chem. Res.*, 2013, **46**, 2396–2406.

25 S. F. Berlanda, M. Breitfeld, C. L. Dietsche and P. S. Dittrich, *Anal. Chem.*, 2021, **93**, 311–331.

26 A. G. Niculescu, C. Chircov, A. C. Bîrcă and A. M. Grumezescu, *Int. J. Mol. Sci.*, 2021, **22**, 1–26.

27 L. J. Pan, J. W. Tu, H. T. Ma, Y. J. Yang, Z. Q. Tian, D. W. Pang and Z. L. Zhang, *Lab Chip*, 2018, **18**, 41–56.

28 X. Zhang and S. J. Haswell, *MRS Bull.*, 2006, **31**, 95–99.

29 D. Sticker, R. Geczy, U. O. Häfeli and J. P. Kutter, *ACS Appl. Mater. Interfaces*, 2020, **12**, 10080–10095.

30 X. Hou, Y. S. Zhang, G. T. De Santiago, M. M. Alvarez, J. Ribas, S. J. Jonas, P. S. Weiss, A. M. Andrews, J. Aizenberg and A. Khademhosseini, *Nat. Rev. Mater.*, 2017, **2**, 1–15.

31 H. Gao, C. Yan, W. Wu and J. Li, *Sensors (Switzerland)*, 2020, **20**, 1792.

32 P. N. Nge, C. I. Rogers and A. T. Woolley, *Chem. Rev.*, 2013, **113**, 2550–2583.

33 J. B. Nielsen, R. L. Hanson, H. M. Almughamsi, C. Pang, T. R. Fish and A. T. Woolley, *Anal. Chem.*, 2020, **92**, 150–168.

34 A. Cignarelli, V. A. Genchi, S. Perrini, A. Natalicchio, L. Laviola and F. Giorgino, *Int. J. Mol. Sci.*, 2019, **20**, 1–20.

35 H. Li and A. J. Steckl, *Anal. Chem.*, 2019, **91**, 352–371.

36 J. P. Rolland, R. M. Van Dam, D. A. Schorzman, S. R. Quake and J. M. DeSimone, *J. Am. Chem. Soc.*, 2004, **126**, 2322–2323.

37 K. W. Bong, J. Lee and P. S. Doyle, *Lab Chip*, 2014, **14**, 4680–4687.

38 R. Jellali, P. Paullier, M. J. Fleury and E. Leclerc, *Sens. Actuators, B Chem.*, 2016, **229**, 396–407.

39 M. Tonin, N. Descharmes and R. Houdré, *Lab Chip*, 2016, **16**, 465–470.

40 C. W. Chang, Y. J. Cheng, M. Tu, Y. H. Chen, C. C. Peng, W. H. Liao and Y. C. Tung, *Lab Chip*, 2014, **14**, 3762–3772.

41 H. J. Chiang, S. L. Yeh, C. C. Peng, W. H. Liao and Y. C. Tung, *J. Vis. Exp.*, 2017, **2017**, 55292.

42 Y. Gao, G. Stybayeva and A. Revzin, *Lab Chip*, 2019, **19**, 306–315.

43 A. Waldbaur, H. Rapp, K. Länge and B. E. Rapp, *Anal. Methods*, 2011, **3**, 2681–2716.

44 C. W. Tsao, *Micromachines*, 2016, **7**, 225.

45 C. Iliescu, H. Taylor, M. Avram, J. Miao and S. Franssila, *Biomicrofluidics*, 2012, **6**, 016505.

46 T. Wang, J. Chen, T. Zhou and L. Song, *Micromachines*, 2018, **9**, 269.

47 Y. Lin, C. Gao, D. Gritsenko, R. Zhou and J. Xu, *Microfluid. Nanofluidics*, 2018, **22**, 97.

48 B. K. Gale, A. R. Jafek, C. J. Lambert, B. L. Goenner, H. Moghimifam, U. C. Nze and S. K. Kamarapu, *Inventions*, 2018, **3**, 60.

49 T. Kilic, F. Navaee, F. Stradolini, P. Renaud and S. Carrara, *Microphysiological Syst.*, 2018, **2**, 1–32

50 N. Azizipour, R. Avazpour, D. H. Rosenzweig, M. Sawan and A. Ajji, *Micromachines*, 2020, **11**, 1–15.

51 A. Aziz, C. Geng, M. Fu, X. Yu, K. Qin and B. Liu, *Bioengineering*, 2017, **4**, 39.

52 N. Wongkaew, M. Simsek, C. Griesche and A. J. Baeumner, *Chem. Rev.*, 2019, **119**, 120–194.

53 S. K. Metkar and K. Girigoswami, *Biocatal. Agric. Biotechnol.*, 2019, **17**, 271–283.

54 G. A. Clarke, B. X. Hartse, A. E. N. Asli, M. Taghavimehr, N. Hashemi, M. A. Shirsavar, R. Montazami, N. Alimoradi, V. Nasirian, L. J. Ouedraogo and N. N. Hashemi, *Sensors*, 2021, **21**, 1–44.

55 S. Patel, R. Nanda, S. Sahoo and E. Mohapatra, Biochem. Res. Int., 2016, **2016**, 3130469.

56 A. B. González-Guerrero, J. Maldonado, S. Herranz and L. M. Lechuga, *Anal. Methods*, 2016, **8**, 8380–8394.

57 J. Wu, M. Dong, C. Rigatto, Y. Liu and F. Lin, *npj Digit. Med.*, 2018, **1**, 7.

58 F. Fontana, J. P. Martins, G. Torrieri and H. A. Santos, *Adv. Mater. Technol.*, 2019, **4**, 1970034.

59 N. Pørksen, B. Nyholm, J. D. Veldhuis, P. C. Butler and O. Schmitz, *Am. J. Physiol.*, 1997, **273**, E908..

60 P. Yao, S. Tung, Z. Zhan, J. Hua and Z. Dong, in *2011 IEEE International Conference on Cyber Technology in Automation, Control, and Intelligent Systems, CYBER 2011*, 2011, pp. 107–111.

61 P. Yao, S. Tung, Z. Zhan, J. Hua and Z. Dong, *Trans. Inst. Meas. Control*, 2013, **35**, 893–900.

62 A. Avoundjian, M. Jalali-Heravi and F. A. Gomez, *Anal. Bioanal. Chem.*, 2017, **409**, 2697–2703.

63 N. Moodley, U. Ngxamngxa, M. J. Turzyniecka and T. S. Pillay, *J. Clin. Pathol.*, 2015, **68**, 258–64.

64 P. Mao and D. Wang, *J. Proteome Res.*, 2014, **13**, 1560–1569.

65 P. Yao, Z. Liu, B. Liu, L. Liu, N. Jiao, Z. Dong and S. Tung, in *2013 IEEE International Conference on Cyber Technology in Automation, Control and Intelligent Systems, IEEE-*

CYBER 2013, **2013**, 149–152.

66 H. Wan, L. Zhuang, Y. Pan, F. Gao, J. Tu, B. Zhang and P. Wang, in *Biomedical Information Technology*, Elsevier, 2020, pp. 51–79.

67 G. C. Ilacas, A. Basa, K. J. Nelms, J. D. Sosa, Y. Liu and F. A. Gomez, *Anal. Chim. Acta*, 2019, **1055**, 74–80.

68 S. Oyola-Reynoso, A. P. Heim, J. Halbertsma-Black, C. Zhao, I. D. Tevis, S. Çınar, R. Cademartiri, X. Liu, J.-F. Bloch and M. M. Thuo, *Talanta*, 2015, **144**, 289–293.

69 P. De Tarso Garcia, T. M. Garcia Cardoso, C. D. Garcia, E. Carrilho and W. K. Tomazelli Coltro, *RSC Adv.*, 2014, **4**, 37637–37644.

70 T. Lam, J. P. Devadhasan, R. Howse and J. Kim, *Sci. Rep.*, 2017, **7**, 1188.

71 E. Evans, E. F. Moreira Gabriel, T. E. Benavidez, W. K. Tomazelli Coltro and C. D. Garcia, *Analyst*, 2014, **139**, 5560–5567.

72 D. Sechi, B. Greer, J. Johnson and N. Hashemi, *Anal. Chem.*, 2013, **85**, 10733–10737.

73 G. Palazzo, L. Facchini and A. Mallardi, *Sens. Actuators, B Chem.*, 2012, **161**, 366–371.

74 A. Kugimiya and E. Matsuzaki, *Appl. Biochem. Biotechnol.*, 2014, **174**, 2527–2536.

75 H. Zhang, E. Smith, W. Zhang and A. Zhou, *Biomed. Microdevices*, 2019, **21**, 48.

76 S. S. Nadar, P. D. Patil, M. S. Tiwari and D. J. Ahirrao, *Crit. Rev. Biotechnol.*, 2021.

77 S. Liu, W. Su and X. Ding, *Sensors*, 2016, **16**, 1–17.

78 Y. A. Yang and C. H. Lin, *Biomicrofluidics*, 2015, **9**, 022402.

79 C.C. Wu, H.I. Lin, K.W. Chang, J. D. Mai, S.C. Shiesh and G.B. Lee, *Microfluid. Nanofluidics*, 2015, **18**, 613–621.

80 E. A. Redman, M. Ramos-Payan, J. S. Mellors and J. M. Ramsey, *Anal. Chem.*, 2016, **88**, 5324–5330.

81 J. Li, K. W. Chang, C. H. Wang, C. H. Yang, S. C. Shiesh and G. Bin Lee, *Biosens. Bioelectron.*, 2016, **79**, 887–893.

82 K. W. Chang, J. Li, C. H. Yang, S. C. Shiesh and G. Bin Lee, *Biosens. Bioelectron.*, 2015, **68**, 397–403.

83 B. Zhang, R. B. Kumar, H. Dai and B. J. Feldman, *Nat. Med.*, 2014, **20**, 948–953.

84 Y. Zhan, D. N. Loufakis, N. Bao and C. Lu, *Lab Chip*, 2012, **12**, 5063–5068.

85 S. Cha, T. Shin, S. S. Lee, W. Shim, G. Lee, S. J. Lee, Y. Kim and J. M. Kim, *Anal. Chem.*, 2012, **84**, 10471–10477.

86 C. H. D. Tsai, S. Sakuma, F. Arai and M. Kaneko, *IEEE Trans. Biomed. Eng.*, 2014, **61**, 1187–1195.

87 D. Bento, R. O. Rodrigues, V. Faustino, D. Pinho, C. S. Fernandes, A. I. Pereira, V. Garcia, J. M. Miranda and R. Lima, *Micromachines*, 2018, **9**, 151.

88 Z. Pu, C. Zou, R. Wang, X. Lai, H. Yu, K. Xu and D. Li, *Biomicrofluidics*, 2016, **10**, 011910.

89 M. Yin, B. Huang, S. Gao, A. P. Zhang and X. Ye, *Biomed. Opt. Express*, 2016, **7**, 2067.

90 A. M. Smink, K. Skrzypek, J. Visser, R. Kuwabara, B. J. de Haan, P. de Vos and D. Stamatialis, *Biomed. Mater.*, 2021, **16**, 035036.

91 V. Iacovacci, L. Ricotti, A. Menciassi and P. Dario, *Biochem. Pharmacol.*, 2016, **100**, 12–27.

92 A. A. Tomei, C. Villa and C. Ricordi, *Expert Opin. Biol. Ther.*, 2015, **15**, 1321–1336.

93 D. Velasco, E. Tumarkin and E. Kumacheva, *Small*, 2012, **8**, 1633–1642.

94 T. Alkayyali, T. Cameron, B. Haltli, R. G. Kerr and A. Ahmadi, *Anal. Chim. Acta*, 2019, **1053**, 1–21.

95 A. A. Tomei, V. Manzoli, C. A. Fraker, J. Giraldo, D. Velluto, M. Najjar, A. Pileggi, R. D. Molano, C. Ricordi, C. L. Stabler and J. A. Hubbell, *Proc. Natl. Acad. Sci. U. S. A.*, 2014, **111**, 10514–10519.

96 U. Barkai, A. Rotem and P. de Vos, *World J. Transplant.*, 2016, **6**, 69.

97 Š. Selimović, J. Oh, H. Bae, M. Dokmeci and A. Khademhosseini, *Polymers*, 2012, **4**, 1554–1579.

98 D. M. Headen, G. Aubry, H. Lu and A. J. García, *Adv. Mater.*, 2014, **26**, 3003–3008.

99 D. M. Headen, J. R. García and A. J. García, *Microsystems Nanoeng.*, 2018, **4**, 1–9.

100 J. D. Weaver, D. M. Headen, M. M. Coronel, M. D. Hunckler, H. Shirwan and A. J.

García, *Am. J. Transplant.*, 2019, **19**, 1315–1327.

101 S. Akbari and T. Pirbodaghi, *Microfluid. Nanofluidics*, 2014, **16**, 773–777.

102 A. G. Håti, D. C. Bassett, J. M. Ribe, P. Sikorski, D. A. Weitz and B. T. Stokke, *Lab Chip*, 2016, **16**, 3718–3727.

103 H. Liu, Y. Wang, H. Wang, M. Zhao, T. Tao, X. Zhang and J. Qin, *Adv. Sci.*, 2020, **7**, 1903739.

104 D. An, A. Chiu, J. A. Flanders, W. Song, D. Shou, Y. C. Lu, L. G. Grunnet, L. Winkel, C. Ingvorsen, N. S. Christophersen, J. J. Fels, F. W. Sand, Y. Ji, L. Qi, Y. Pardo, D. Luo, M. Silberstein, J. Fan and M. Ma, *Proc. Natl. Acad. Sci. U. S. A.*, 2017, **115**, E263–E272.

105 T. Watanabe, T. Okitsu, F. Ozawa, S. Nagata, H. Matsunari, H. Nagashima, M. Nagaya, H. Teramae and S. Takeuchi, *Biomaterials*, 2020, **255**, 120162.

106 J. Cheng, Y. Jun, J. Qin and S. H. Lee, *Biomaterials*, 2017, **114**, 121–143.

107 K. H. Lee, S. J. Shin, Y. Park and S. H. Lee, *Small*, 2009, **5**, 1264–1268.

108 Y. Jun, M. J. Kim, Y. H. Hwang, E. A. Jeon, A. R. Kang, S. H. Lee and D. Y. Lee, *Biomaterials*, 2013, **34**, 8122–8130.

109 Y. Jun, A. R. Kang, J. S. Lee, G. S. Jeong, J. Ju, D. Y. Lee and S. H. Lee, *Biomaterials*, 2013, **34**, 3784–3794.

110 Y. Jun, A. R. Kang, J. S. Lee, S. J. Park, D. Y. Lee, S. H. Moon and S. H. Lee, *Biomaterials*, 2014, **35**, 4815–4826.

111 H. Onoe, T. Okitsu, A. Itou, M. Kato-Negishi, R. Gojo, D. Kiriya, K. Sato, S. Miura, S. Iwanaga, K. Kuribayashi-Shigetomi, Y. T. Matsunaga, Y. Shimoyama and S. Takeuchi, *Nat. Mater.*, 2013, **12**, 584–590.

112 A. Soltani, M. Soleimani, M. A. Ghiass, S. E. Enderami, S. Rabbani, A. Jafarian and A. Allameh, *Life Sci.*, 2021, **274**, 119338.

113 F. Ozawa, T. Okitsu and S. Takeuchi, *ACS Biomater. Sci. Eng.*, 2017, **3**, 392–398.

114 S. N. Bhatia and D. E. Ingber, *Nat. Biotechnol.*, 2014, **32**, 760–772.

115 A. Polini, L. Prodanov, N. S. Bhise, V. Manoharan, M. R. Dokmeci and A. Khademhosseini, *Expert Opin. Drug Discov.*, 2014, **9**, 335–352.

116 H. Kimura, Y. Sakai and T. Fujii, *Drug Metab. Pharmacokinet.*, 2018, **33**, 43–48.

117 A. Zbinden, J. Marzi, K. Schlünder, C. Probst, M. Urbanczyk, S. Black, E. M. Brauchle, S. L. Layland, U. Kraushaar, G. Duffy, K. Schenke-Layland and P. Loskill, *Matrix Biol.*, 2020, **85**–**86**, 205–220.

118 S. Abadpour, A. Aizenshtadt, P. A. Olsen, K. Shoji, S. R. Wilson, S. Krauss and H. Scholz, *Curr. Diab. Rep.*, 2020, **20**, 1–13.

119 Y. Jun, J. S. Lee, S. Choi, J. H. Yang, M. Sander, S. Chung and S. H. Lee, *Sci. Adv.*, 2019, **5**, 4520–4547.

120 Y. Yu, A. Gamble, R. Pawlick, A. R. Pepper, B. Salama, D. Toms, G. Razian, C. Ellis, A. Bruni, B. Gala-Lopez, J. L. Lu, H. Vovko, C. Chiu, S. Abdo, T. Kin, G. Korbutt, A. M. J. Shapiro and M. Ungrin, *Diabetologia*, 2018, **61**, 2016–2029.

121 P. L. Lewis and J. M. Wells, *Stem Cells*, 2021, **39**, 522–535.

122 J. S. Mohammed, Y. Wang, T. A. Harvat, J. Oberholzer and D. T. Eddington, *Lab Chip*, 2009, **9**, 97–106.

123 T. Schulze, K. Mattern, E. Früh, L. Hecht, I. Rustenbeck and A. Dietzel, *Biomed. Microdevices*, 2017, **19**, 1–11.

124 T. Schulze, K. Mattern, P. Erfle, D. Brüning, S. Scherneck, A. Dietzel and I. Rustenbeck, *Front. Bioeng. Biotechnol.*, 2021, **9**, 158.

125 T. Tao, Y. Wang, W. Chen, Z. Li, W. Su, Y. Guo, P. Deng and J. Qin, *Lab Chip*, 2019, **19**, 948–958.

126 A. Essaouiba, T. Okitsu, R. Jellali, M. Shinohara, M. Danoy, Y. Tauran, C. Legallais, Y. Sakai and E. Leclerc, *Mol. Cell. Endocrinol.*, 2020, **514**, 110892.

127 K. Hirano, S. Konagaya, A. Turner, Y. Noda, S. Kitamura, H. Kotera and H. Iwata, *Biochem. Biophys. Res. Commun.*, 2017, **487**, 344–350.

128 L. J. Y. Ong, L. H. Chong, L. Jin, P. K. Singh, P. S. Lee, H. Yu, A. Ananthanarayanan, H. L. Leo and Y. C. Toh, *Biotechnol. Bioeng.*, 2017, **114**, 2360–2370.

129 S. H. Lee, S. G. Hong, J. Song, B. Cho, E. J. Han, S. Kondapavulur, D. Kim and L. P. Lee, *Adv. Healthc. Mater.*, 2018, **7**, 1701111.

130 A. Essaouiba, R. Jellali, M. Shinohara, B. Scheidecker, C. Legallais, Y. Sakai and E. Leclerc, *J. Biotechnol.*, 2021, **330**, 45–56.

131 T. Hori, K. Yamane, T. Anazawa, O. Kurosawa and H. Iwata, *Biomed. Microdevices*, 2019, **21**, 1–9.

132 K. S. Sankar, B. J. Green, A. R. Crocker, J. E. Verity, S. M. Altamentova and J. V. Rocheleau, *PLoS One*, 2011, **6**, e24904.

133 P. N. Silva, B. J. Green, S. M. Altamentova and J. V. Rocheleau, *Lab Chip*, 2013, **13**, 4374–4384.

134 A. L. Glieberman, B. D. Pope, J. F. Zimmerman, Q. Liu, J. P. Ferrier, J. H. R. Kenty, A. M. Schrell, N. Mukhitov, K. L. Shores, A. B. Tepole, D. A. Melton, M. G. Roper and K. K. Parker, *Lab Chip*, 2019, **19**, 2993–3010.

135 M. Nourmohammadzadeh, Y. Xing, J. W. Lee, M. A. Bochenek, J. E. Mendoza-Elias, J. J. McGarrigle, E. Marchese, Y. Chun-Chieh, D. T. Eddington, J. Oberholzer and Y. Wang, *Lab Chip*, 2016, **16**, 1466–1472.

136 D. Balboa, J. Saarimäki-Vire and T. Otonkoski, *Stem Cells*, 2019, **37**, 33–41.

137 R. Scharfmann, W. Staels and O. Albagli, *J. Clin. Invest.*, 2019, **129**, 3511–3520.

138 A. D. Green, S. Vasu, R. C. Moffett and P. R. Flatt, *Biochimie*, 2016, **125**, 119–125.

139 D. T. T. Nguyen, D. Van Noort, I. K. Jeong and S. Park, *Biofabrication*, 2017, **9**, 015021.

140 J. Y. Kim, H. W. Kim, S. J. Bae, D. J. Joo, K. H. Huh, Y. H. Fang, Y. Cho, J. H. Jeong, Y. S. Kim and J. I. Lee, in *Transplantation Proceedings*, Elsevier, 2012, **44**, 1095–1098.

141 S. G. Yabe, S. Fukuda, F. Takeda, K. Nashiro, M. Shimoda and H. Okochi, *J. Diabetes*, 2017, **9**, 168–179.

142 S. G. Yabe, S. Fukuda, J. Nishida, F. Takeda, K. Nashiro and H. Okochi, *Regen. Ther.*, 2019, **10**, 69–76.

143 N. S. Amirruddin, B. S. J. Low, K. O. Lee, E. S. Tai and A. K. K. Teo, *Semin. Cell Dev. Biol.*, 2020, **103**, 31–40.

144 M. Bakhti, A. Böttcher and H. Lickert, *Nat. Rev. Endocrinol.*, 2019, **15**, 155–171.

145 V. Volarevic, B. S. Markovic, M. Gazdic, A. Volarevic, N. Jovicic, N. Arsenijevic, L.

Armstrong, V. Djonov, M. Lako and M. Stojkovic, *Int. J. Med. Sci.*, 2018, **15**, 36–45.

146 S. Zhu, H. A. Russ, X. Wang, M. Zhang, T. Ma, T. Xu, S. Tang, M. Hebrok and S. Ding, *Nat. Commun.*, 2016, **7**, 1–13.

147 S. Kahraman, E. R. Okawa and R. N. Kulkarni, *Curr. Diab. Rep.*, 2016, **16**, 1–8.

148 M. Hohwieler, M. Müller, P. O. Frappart and S. Heller, *Stem Cells Int.*, 2019, **2019**, 9301382.

149 K. S. Polonsky, B. D. Given and E. Van Cauter, *J. Clin. Invest.*, 1988, **81**, 442–448.

150 Y. Wang, J. F. Lo, J. E. Mendoza-Elias, A. F. Adewola, T. A. Harvat, K. P. Kinzer, D. Lee, M. Qi, D. T. Eddington and J. Oberholzer, *Bioanalysis*, 2010, **2**, 1729–1744.

151 P. M. Misun, B. Yesildag, F. Forschler, A. Neelakandhan, N. Rousset, A. Biernath, A. Hierlemann and O. Frey, *Adv. Biosyst.*, 2020, **4**, 1900291.

152 M. A. Ortega, J. Rodríguez-Comas, O. Yavas, F. Velasco-Mallorquí, J. Balaguer-Trias, V. Parra, A. Novials, J. M. Servitja, R. Quidant and J. Ramón-Azcón, *Biosensors*, 2021, **11**, 138.

153 R. Perrier, A. Pirog, M. Jaffredo, J. Gaitan, B. Catargi, S. Renaud, M. Raoux and J. Lang, *Biosens. Bioelectron.*, 2018, **117**, 253–259.

154 J. F. Dishinger and R. T. Kennedy, *Anal. Chem.*, 2007, **79**, 947–954.

155 J. F. Dishinger, K. R. Reid and R. T. Kennedy, *Anal. Chem.*, 2009, **81**, 3119–3127.

156 A. F. Adewola, Y. Wang, T. Harvat, D. T. Eddington, D. Lee and J. Oberholzer, *J. Vis. Exp.*, 2010, **26**, 1649.

157 Y. Xing, M. Nourmohammadzadeh, J. E. M. Elias, M. Chan, Z. Chen, J. J. McGarrigle, J. Oberholzer and Y. Wang, *Biomed. Microdevices*, 2016, **18**, 1–9.

158 L. S. Satin, P. C. Butler, J. Ha and A. S. Sherman, *Mol. Aspects Med.*, 2015, **42**, 61–77.

159 M. C. Beauvois, C. Merezak, J. C. Jonas, M. A. Ravier, J. C. Henquin and P. Gilon, *Am. J. Physiol. - Cell Physiol.*, 2006, **290**, 1503–1511.

160 J. A. Lees, M. Messa, E. W. Sun, H. Wheeler, F. Torta, M. R. Wenk, P. De Camilli and K. M. Reinisch, *Science*, 2017, **355**, 6171.

161 S. N. Patel, M. Ishahak, D. Chaimov, A. Velraj, D. LaShoto, D. W. Hagan, P. Buchwald,

E. A. Phelps, A. Agarwal and C. L. Stabler, *Sci. Adv.*, 2021, **7**, 5515–5527.

162 R. P. Robertson, J. Harmon, P. O. T. Tran and V. Poitout, in *Diabetes*, American Diabetes Association Inc., 2004, **53**, S119–S124.

163 K. S. Park, Y. S. Kim, J. H. Kim, B. K. Choi, S. H. Kim, S. H. Oh, Y. R. Ahn, M. S. Lee, M. K. Lee, J. B. Park, C. H. Kwon, J. W. Joh, K. W. Kim and S. J. Kim, *Transplant. Proc.*, 2009, **41**, 3813–3818.

164 J. Chen, Y. F. Ye, L. M. Liao, J. Q. Cai, L. H. Huang, S. L., Y. J. Ma, Y. F. Fu, X. M. Xu and J. M. Tan, *CellR4,* 2013, **1**, e382.

165 P. Lin, L. Chen, D. Li, N. Yang, Y. Sun and Y. Xu, *Neuroendocrinol. Lett.*, 2009, **30**, 204–208.

166 M. Brissova and A. C. Powers, *Diabetes*, 2008, **57**, 2269–2271.

167 L. Jansson and P. O. Carlsson, *Diabetologia*, 2002, **45**, 749–763.

168 D. Nyqvist, M. Köhler, H. Wahlstedt and P. O. Berggren, *Diabetes*, 2005, **54**, 2287–2293.

169 W. Hong, S. Lin, M. Zippi, W. Geng, S. Stock, Z. Basharat, B. Cheng, J. Pan and M. Zhou, *Can. J. Gastroenterol. Hepatol.*, 2017, **2017**, 5297143.

170 K. S. Sankar, S. M. Altamentova and J. V. Rocheleau, *PLoS One*, 2019, **14**, e0222424.

171 L. A. Godwin, J. C. Brooks, L. D. Hoepfner, D. Wanders, R. L. Judd and C. J. Easley, *Analyst*, 2015, **140**, 1019–1025.

172 J. C. Brooks, K. I. Ford, D. H. Holder, M. D. Holtan and C. J. Easley, *Analyst*, 2016, **141**, 5714–5721.

173 X. Li, J. C. Brooks, J. Hu, K. I. Ford and C. J. Easley, *Lab Chip*, 2017, **17**, 341–349.

174 S. Seino, K. Sugawara, N. Yokoi and H. Takahashi, *Diabetes, Obes. Metab.*, 2017, **19**, 22–29.

175 K. Ramachandran, S. J. Williams, H. H. Huang, L. Novikova and L. Stehno-Bittel, *Tissue Eng. - Part A*, 2013, **19**, 604–612.

176 R. Ritzel, M. Schulte, N. Pørksen, M. S. Nauck, J. J. Holst, C. Juhl, W. März, O. Schmitz, W. H. Schmiegel and M. A. Nauck, *Diabetes*, 2001, **50**, 776–784.

177 N. Gupta, J. R. Liu, B. Patel, D. E. Solomon, B. Vaidya and V. Gupta, *Bioeng. Transl. Med.*, 2016, **1**, 63–81.

178 S. Bauer, C. Wennberg Huldt, K. P. Kanebratt, I. Durieux, D. Gunne, S. Andersson, L. Ewart, W. G. Haynes, I. Maschmeyer, A. Winter, C. Ämmälä, U. Marx and T. B. Andersson, *Sci. Rep.*, 2017, **7**, 1–11.

179 J. Bailey, M. Thew and M. Balls, *ATLA Altern. to Lab. Anim.*, 2013, **41**, 335–350.

180 N. Gaio, B. van Meer, W. Q. Solano, L. Bergers, A. van de Stolpe, C. Mummery, P. M. Sarro and R. Dekker, *Micromachines*, 2016, **7**, 120.

181 N. Picollet-D'hahan, A. Zuchowska, I. Lemeunier and S. Le Gac, *Trends Biotechnol.*, 2021, https://doi.org/10.1016/j.tibtech.2020.11.014.

182 Y. Zhao, R. K. Kankala, S. Bin Wang and A. Z. Chen, *Molecules*, 2019, 24, 675.

183 Q. Wu, J. Liu, X. Wang, L. Feng, J. Wu, X. Zhu, W. Wen and X. Gong, *Biomed. Eng. Online*, 2020, **19**, 1–19.

184 A. Essaouiba, T. Okitsu, R. Kinoshita, R. Jellali, M. Shinohara, M. Danoy, C. Legallais, Y. Sakai and E. Leclerc, *Biochem. Eng. J.*, 2020, **164**, 107783.

185 D. W. Lee, S. H. Lee, N. Choi and J. H. Sung, *Biotechnol. Bioeng.*, 2019, **116**, 3433–3445.

186 O. Pivovarova, W. Bernigau, T. Bobbert, F. Isken, M. Möhlig, J. Spranger, M. O. Weickert, M. Osterhoff, A. F. H. Pfeiffer and N. Rudovich, *Diabetes Care*, 2013, **36**, 3779–3785.

187 S. Lu, C. E. Dugan and R. T. Kennedy, *Anal. Chem.*, 2018, **90**, 5171–5178.

188 Y. Ohmura, M. Tanemura, N. Kawaguchi, T. MacHida, T. Tanida, T. Deguchi, H. Wada, S. Kobayashi, S. Marubashi, H. Eguchi, Y. Takeda, N. Matsuura, T. Ito, H. Nagano, Y. Doki and M. Mori, *Transplantation*, 2010, **90**, 1366–1373.

189 O. Yesil-Celiktas, O. Hassan, A. K. Miri, S. Maharjan, R. Al-kharboosh, A. Quiñones-Hinojosa and Y. S. Zhang, *Adv. Biosys.*, 2018, **2**, 1800109.

190 Y.Liu, E. Gill and Y. Y. Shery Huang, *Future Sci OA*, 2017, **3**, FSO173.

191 M. Ruoß, M. Vosough, A. Königsrainer, S. Nadalin, S. Wagner, S. Sajadian, D. Huber,

Z. Heydari, S. Ehnert, J. G. Hengstler and A. K. Nussler, *Food Chem. Toxicol.*, 2020, **138**, 111188.

192 H. G. Yi, H. Lee and D. W. Cho, *Bioengineering*, 2017, **4**, 10.

193 K. Duval, H. Grover, L. H. Han, Y. Mou, A. F. Pegoraro, J. Fredberg and Z. Chen, *Physiology*, 2017, **32**, 266–277.

194 N. S. Bhise, V. Manoharan, S. Massa, A. Tamayol, M. Ghaderi, M. Miscuglio, Q. Lang, Y. Shrike Zhang, S. R. Shin, G. Calzone, N. Annabi, T. D. Shupe, C. E. Bishop, A. Atala, M. R. Dokmeci and A. Khademhosseini, *Biofabrication*, 2016, **8**, 014101.

195 H. Lee, S. Chae, J. Y. Kim, W. Han, J. Kim, Y. Choi and D. W. Cho, *Biofabrication*, 2019, **11**, 025001.

196 Y. Zhang, N. Yang, L. Xie, F. Shu, Q. Shi and N. Shaheen, *Micromachines*, 2020, **11**, 1118.

197 Q. Meng, Y. Wang, Y. Li and C. Shen, *Biotechnol. Bioeng.,* 2021, **118**, 612– 621.

198 L. Boulais, R. Jellali, U. Pereira, E. Leclerc, S. A. Bencherif and C. Legallais, 2020, http://dx.doi.org/10.2139/ssrn.3757905.

199 G. Agrawal, A. Aung and S. Varghese, *Lab Chip*, 2017, **17**, 3447– 3461.

200 K. Shimizu, H. Araki, K. Sakata, W. Tonomura, M. Hashida and S. Konishi, *J Biosci Bioeng.*, 2015, **119**, 212–216.

201 C. G. Anene-Nzelu, K. Y. Peh, A. Fraiszudeen, Y. H. Kuan, S. H. Ng, Y. C. Toh, H. L. Leo and H. Yu, *Lab Chip*. 2013, **13**, 4124–4133.

202 F. Yang, A. Carmona, K. Stojkova, E. I. Garcia Huitron, A. Goddi, A. Bhushan, R. N. Cohen and E. M. Brey, *Lab Chip*, 2021, **21**, 435–446.

203 J. Rogal, C. Binder, E. Kromidas, J. Roosz, C. Probst, S. Schneider, K. Schenke-Layland and P. Loskill, *Sci. Rep.*, 2020, **10**, 6666.

Table 1. Summary of LoC-based technologies developed for DM diagnosis and management

Target Analyte	Technology (group)	Technique	Assay time	LOD*	Sample volume	Detector	Ref
Glucose	Paper µPAD	Colorimetric immunoassay	20 min	-	3 µL	Hp Scanjet 6300c	72
Glucose	Paper µPAD (silica nanoparticles)	Colorimetric immunoassay	30 min	0.5 mM	10 µL	Flatbed scanner	71
Glucose	Paper µPAD	Colorimetric immunoassay	2-3.5 h	0.25 mmol/L	40 µL	Epson Perfection V600	67
Glucose	Paper µPAD	Colorimetric immunoassay	5 min	0.01 mg/ml	15 µl	Epson Perfection V19	75
Glucose	Paper µPAD	Colorimetric immunoassay	10 min	13 mg/dL	5 µL	-	70
Glucose	Paper µPAD (silane/hexane ink)	Colorimetric immunoassay	94 min	5.5 mM	-	Desktop scanner	68
Glucose	Paper µPAD	Colorimetric immunoassay	10 min	0.7 mmol/l	40 µL	Hewlett–Packard, model F4280	69
Glucose	Optical gold nanoparticles Assay	Colorimetric immunoassay		5 µM		Absorbance reader	73
Glucose	Integrated electrode	Electrochemical sensor	Online	1.44 mg/dl	-	Ammeter	88
Glucose	Enzyme-doped thread	Electrochemical sensor	-	0.1mM	2 µL	Ammeter	78
Glucose	long-period grating sensor	Optical fiber sensor	Online	10 µM	-	Wavelength detector	89
HbA1c Glycated HSA apoA-I	Multinozzle emitter array chip	Top-down proteomics	2.5 h	-	10 µL	Mass spectrometer	64
HbA1c Glycated HSA	-	Capillary electrophoresis & mass spectrometry	-	-	10 µL	Mass spectrometer	80
HbA1c	Chemiluminescent aptamer–antibody sandwich assay	Nucleic-acid based aptamer	25 min	-	50 µL	Luminometer	82
HbA1c	Chemiluminescent antibody sandwich assay	Antibody-based automated chip	15 min	-	1 µL	Luminometer	79
HbA1c Total Hb	aptamer–antibody sandwich assay	Antibody-based automated chip	30 min	-	100 µL	Photomultiplier tube	81

Serine	-	Enzymatic reaction	30 min	2 mM	250 mM	Thermal lens detector	74
RBC fragility	-	Osmotic lysis kinetics	-	5 mM	-	CDD camera + Microscope	84
RBC deformability	-	Viscoelastic particle focusing	-	-	-	Optical microscope	85
RBC deformability	-	Equilibrium velocity of a cell in a microchannel	-	-	-	Optical microscope	86
Insulin	PDMS device	Chemiluminescent assay	10 min	4×10^{-10} mol/l	-	Photometer	65
insulin, GAD65 IA2	plasmonic gold substrate for NIR-FE detection	Plasmonic Chip	2 h		2 µL	Licor Odyssey scanner	83

* Limit of detection

Table 2. Applications and characteristics of main pancreas-on-chip models reported in literature.

Purpose	Type of cells	Species	Biochips design	Aspect study	Ref
Islet evaluation	Pancreatic islets	Human Mouse	Chamber with microwells	Cell viability and morphology, GSIS, insulin secretion, mitochondrial potential, intracellular calcium	122
Islet evaluation	alpha and bêta-cells derived from iPSC	Human	Multilayer device	Cell viability and morphology, expression of islets-specific genes and proteins, GSIS, insulin secretion, intracellular calcium	125
Islet evaluation	Pancreatic islets	Mouse	Chamber with microwells	Islet functionality under glucose gradients (insulin secretion, mitochondrial potential, intracellular calcium)	156
Islet evaluation	Pancreatic islets and adipose tissue	Mouse	Microchamber with 3D-printed PLA template interface	GSIS, glycerol secretion	172
Islets evaluation and preservation	Pancreatic islets and endothelial cells	Mouse	Microchamber	Cell viability and morphology, islets functions under glucose gradients (insulin secretion, intracellular calcium and membrane depolarization)	132
Islets evaluation	Pancreatic islets and stem cell-derived beta cells	Human	Trapping sites	Automated measurement of glucose-stimulated insulin secretion	134
Islets evaluation	Pancreatic islets and adipose tissue	Mouse	Microchamber with 3D-templated tissue culture interface	Dynamic and quantitative measurements of both hormone secretion and nutrient sensing/uptake	173
Islets preservation	Pancreatic islets and bone marrow mesenchymal stem cells	Rat	Microchamber	Cell migration and insulin secretion in response to high-glucose-challenge	165
Islets evaluation	Pancreatic islets	Mouse	Microstructured borosilicate glass	Oxygen consumption, NADPH autofluorescence, intracellular calcium, insulin secretion	123
Islets evaluation	EndoC-βH3	Human	Trapping sites	Cell viability, GSIS, insulin secretion, mitochondrial activity	117
Islets preservation and physiology	Pancreatic islets within 3D alginate hydrogel	Human Mouse	Microchamber	In situ tracking of viability and calcium signalling, oxygen gradient, oxidative stress under glucolipotoxicity environment, GSIS	161
Islets evaluation and physiology	Pancreatic islets	Human Mouse	Pumpless biochip with trapping sites	Insulin secretion kinetics under glucose stimulation, intracellular calcium oscillation	157
Islets physiology	Pancreatic islets	Mouse	Cellulose-base scaffold	In situ insulin monitoring, GSIS, expression of islets-specific genes	152

Islets physiology	Pancreatic β-cells	Human	Microchamber	Beta cells spheroids formation, oxidative stress under glucolipotoxicity environement, intracellular calcium	129
Islets physiology	Pancreatic islets	Mouse	Symmetric and anti-parallel chambers	Islets activity, continuous glucose monitoring	153
Islets physiology	Pancreatic islets	Mouse	Independant channel networks	Continuous monitoring of glucose-stimulated insulin secretion	154
Islets physiology	Pancreatic islets	Mouse	Independant microchamber	Automated measurement of glucose-stimulated insulin secretion, effect of lipotoxicity environment on intracellular calcium and insulin secretion	155
Islets evaluation, physiology and drug screening	Reagregatted islets	Human	Microfluidic hanging-drop biochip	Dynamics of insulin release at high temporal resolution	151
Islets functions and drug screening	Pancreatic islets	Rat	Concave microwells	Cell viability, ultrastructure morphology, expression of islets-specific genes and proteins, GSIS, drugs screening	119
Islets functions and drug screening	hiPSCs derived β-cells	Human	Crest and honeycombs wells	Cell viability, expression of islets-specific genes and proteins, GSIS, insulin and C-peptide secretion, GLP-1 stimulation	130
Islets functions and drug screening	Pancreatic islets	Rat	Flat microwells	Islet viability, expression of islets-specific genes and proteins, GSIS, insulin, glucagon and C-peptide secretion, GLP-1 stimulation	126

Figure 1. Mechanisms of glycemia regulation by the pancreas and other tissues under normal and diabetic conditions.

Figure 2. Schematic illustration of the main fabrication methods used in microfluidic devices manufacturing.

Figure 3. Schematic overview of the components of a biosensor integrated in a LoC platform.

Figure 4. Microfluidic platforms for islets/β-cells encapsulation. (A) microfluidic co-flow device and (B) parallel droplet generators on a two-layer microfluidic device for small-sized monodisperse microcapsules production; (C) double coaxial microfluidic device and (D) cylindrical and coaxial-flow channels used for islets and β-cells encapsulation in microfibers (reproduced with permission from A: Håti et *al.,* 2016 [102]; B: Headen et *al.,* 2018 [99]; C: Watanabe et *al.,* 2020 [105]; D: Jun et *al.,* 2013 [108]).

Figure 5. Geometric designs used for islets/pseudo-islets trapping in microfluidic devices under flow. (A) microwells; (B) crescent-shaped structures; (C) nozzle system or channel reduction and (D) geometric constructions using hydrodynamic trapping principle (reproduced with permission from A: Tao et al., 2019 [125]; B: Essaouiba et *al.,* 2021 [130]; C: Silva et al., 2013 [133]; D: Zbinden et *al.,* 2020 [117])

Figure 6. Advantages and limitations of the potential cell sources for *in vitro* pancreas-on-chip models (DE: definitive endoderm, PE: pancreatic endoderm and EP: endocrine progenitor).

Figure 7. Main organs involved in T2DM (adapted from Rogal et *al.,* 2019 [11]).

Figure 8. Multiorgan-on-chip models for liver/pancreas interaction studies: (A) microphysiological two-organ-chip (2-OC) device developed by TissUse GmbH (Berlin, Germany) for human pancreatic islets/HepaRG spheroids study; (B) setup used by Essaouiba et *al.,* to study crosstalk between rat islets/rat primary hepatocytes (reproduced with permission from A: Bauer et *al.,* 2017 [178]; B: Essaouiba et *al.,* 2020 [184]).

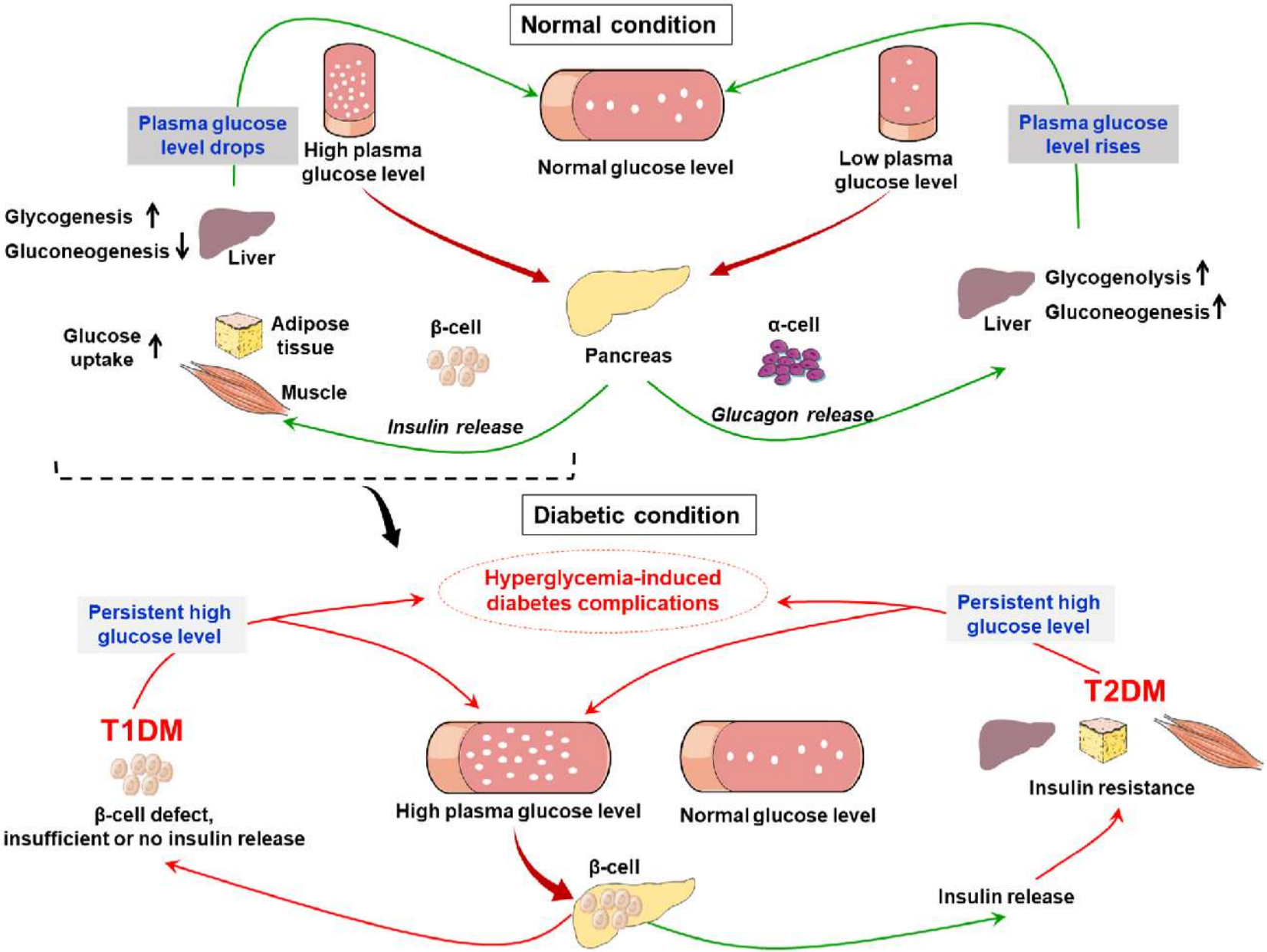
Normal condition
Plasma glucose level drops
High plasma glucose level
Normal glucose level
Low plasma glucose level
Plasma glucose level rises
Glycogenesis
Gluconeogenesis
Liver
Glycogenolysis
Gluconeogenesis
Liver
Glucose uptake
Adipose tissue
Muscle
β-cell
Pancreas
α-cell
Insulin release
Glucagon release
Diabetic condition
Hyperglycemia-induced diabetes complications
Persistent high glucose level
Persistent high glucose level
T1DM
T2DM
β-cell defect, insufficient or no insulin release
High plasma glucose level
Normal glucose level
Insulin resistance
β-cell
Insulin release

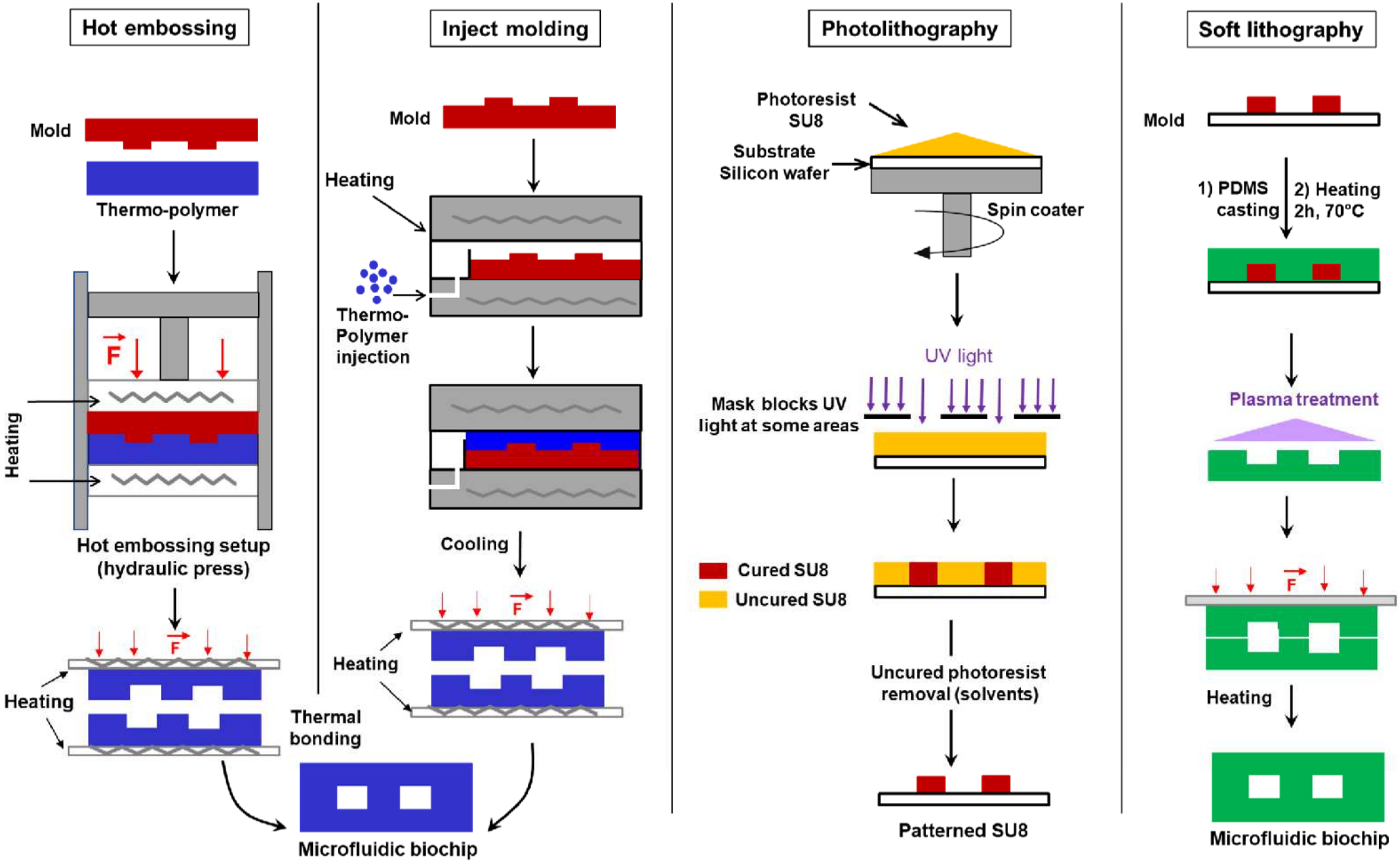
Hot embossing
Mold
Thermo-polymer
F
Heating
Hot embossing setup
(hydraulic press)
F
Heating
Thermal
bonding
Microfluidic biochip
Inject molding
Mold
Heating
Thermo-
Polymer
injection
Cooling
F
Heating
Photolithography
Photoresist
SU8
Substrate
Silicon wafer
Spin coater
UV light
Mask blocks UV
light at some areas
Cured SU8
Uncured SU8
Uncured photoresist
removal (solvents)
Patterned SU8
Soft lithography
Mold
1) PDMS
casting
2) Heating
2h, 70°C
Plasma treatment
F
Heating
Microfluidic biochip

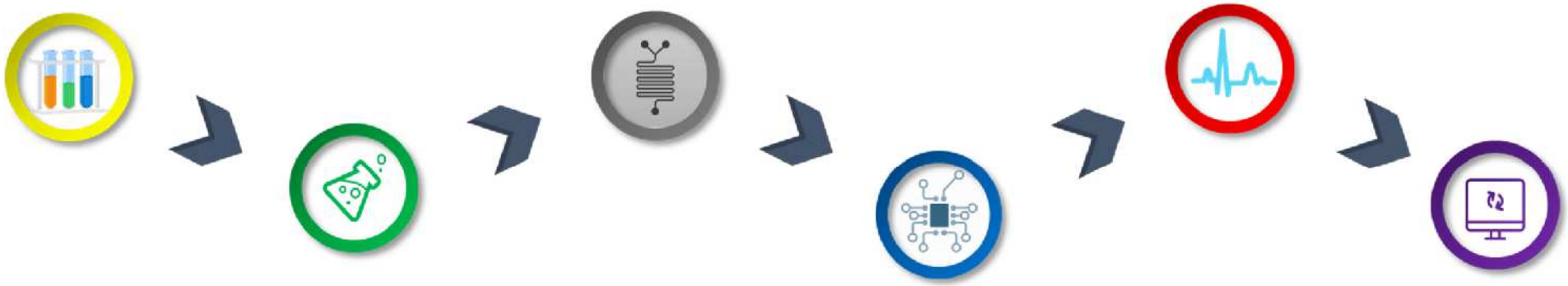

Sample

Human: blood, plasma, saliva, tear, urine or sweat
Cell culture: supernatant or culture media

Analyte

biomarkers, toxins, metabolites, pathogens, hormones…

Bioreceptor

Enzymes, antibodies, aptamers, nucleic acids or cells

Transducer

Opticals, piezoelectrics, calorimetrics, electrochemicals, acoustics…

Signal

Conversion, filtering and amplification: potenciometry, impedance, voltometry, conductometry

Display

Signal processing and display

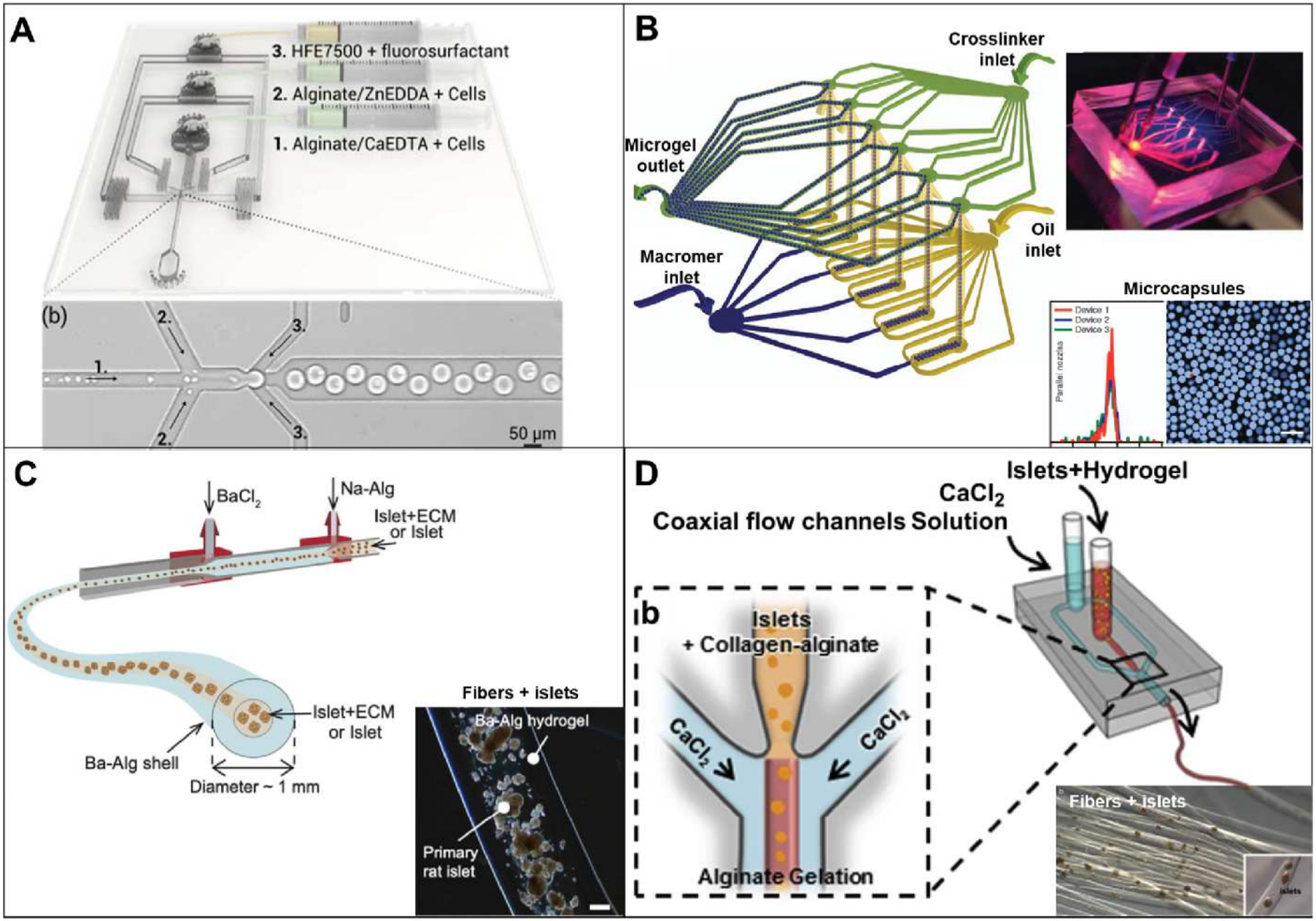
A
3. HFE7500 + fluorosurfactant
2. Alginate/ZnEDDA + Cells
1. Alginate/CaEDTA + Cells
(b)
1.
2.
3.
50 μm
B
Crosslinker inlet
Microgel outlet
Oil inlet
Macromer inlet
Microcapsules
Device 1
Device 2
Device 3
Parallel nozzles
C
$BaCl_2$
Na-Alg
Islet+ECM or Islet
Islet+ECM or Islet
Ba-Alg shell
Diameter ~ 1 mm
Fibers + islets
Ba-Alg hydrogel
Primary rat islet
D
Islets+Hydrogel
$CaCl_2$
Coaxial flow channels Solution
b
Islets
+ Collagen-alginate
$CaCl_2$
$CaCl_2$
Alginate Gelation
Fibers + islets
islets

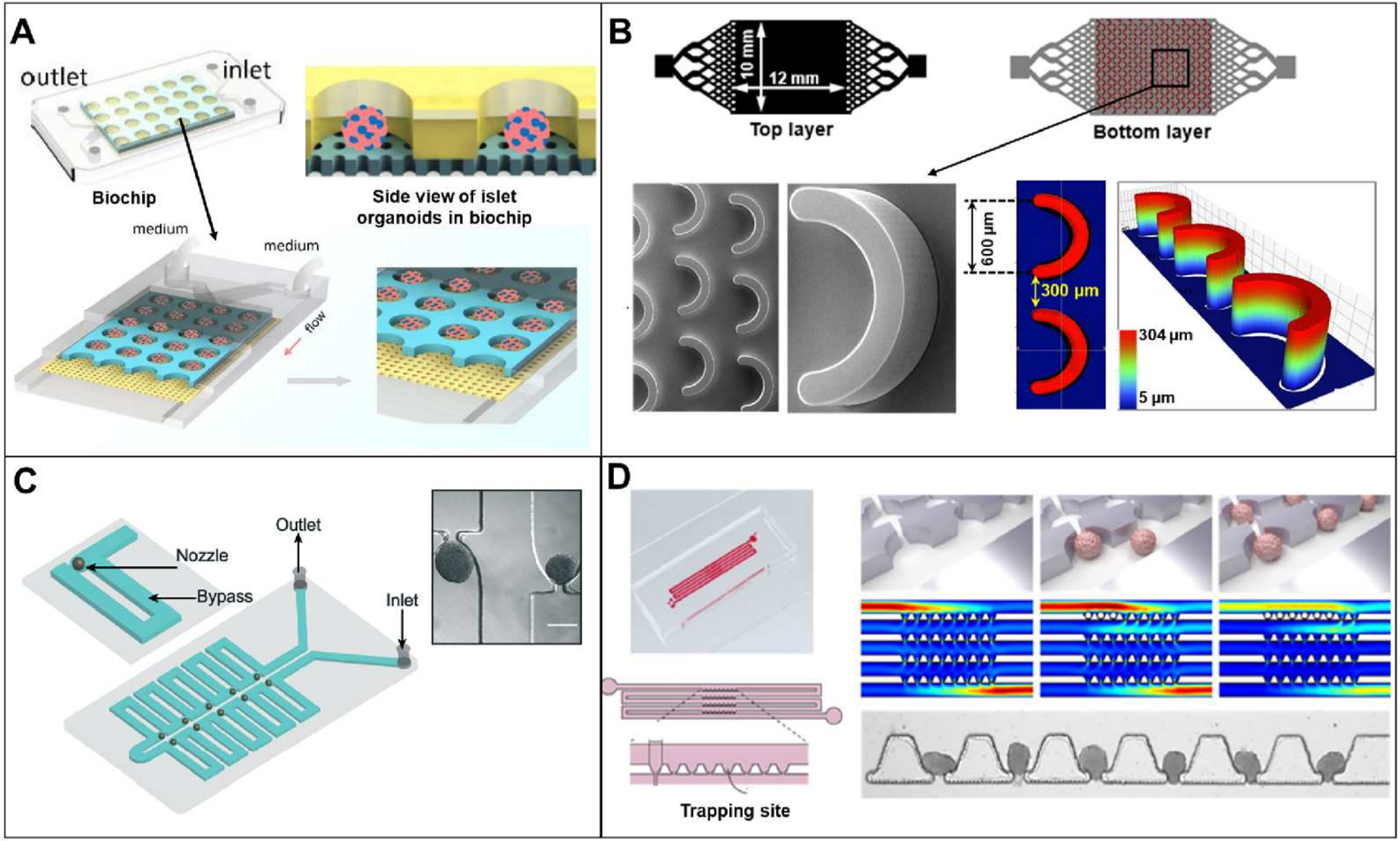
A
outlet
inlet
Biochip
Side view of islet organoids in biochip
medium
medium
flow
B
10 mm
12 mm
Top layer
Bottom layer
600 µm
300 µm
304 µm
5 µm
C
Outlet
Nozzle
Bypass
Inlet
D
Trapping site

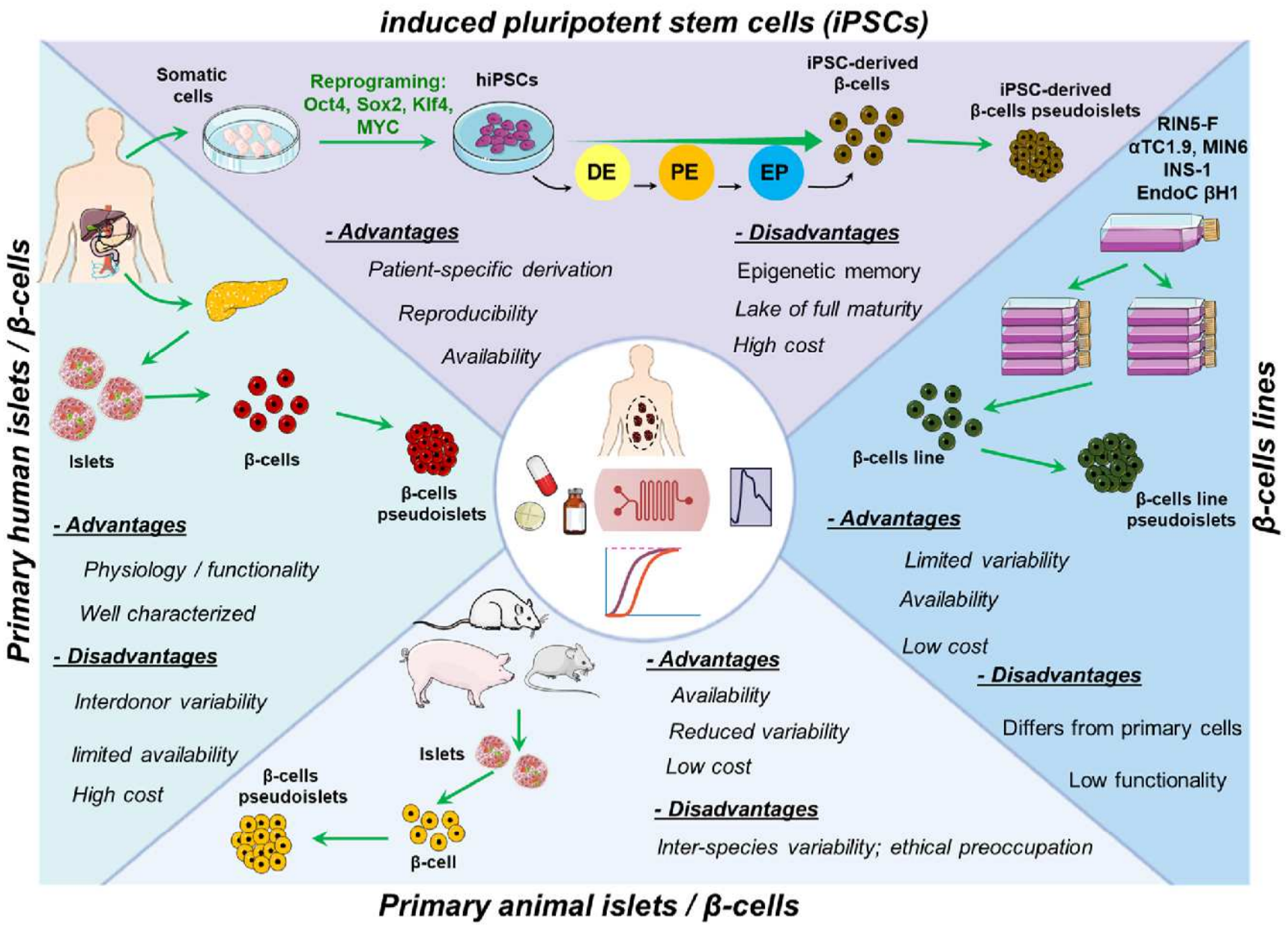
induced pluripotent stem cells (iPSCs)
Somatic cells
Reprograming: Oct4, Sox2, Klf4, MYC
hiPSCs
DE
PE
EP
iPSC-derived β-cells
iPSC-derived β-cells pseudoislets
- Advantages
Patient-specific derivation
Reproducibility
Availability
- Disadvantages
Epigenetic memory
Lake of full maturity
High cost
RIN5-F
αTC1.9, MIN6
INS-1
EndoC βH1
Primary human islets / β-cells
Islets
β-cells
β-cells pseudoislets
- Advantages
Physiology / functionality
Well characterized
- Disadvantages
Interdonor variability
limited availability
High cost
β-cells line
β-cells line pseudoislets
- Advantages
Limited variability
Availability
Low cost
- Disadvantages
Differs from primary cells
Low functionality
β-cells lines
- Advantages
Availability
Reduced variability
Low cost
- Disadvantages
Inter-species variability; ethical preoccupation
Islets
β-cells pseudoislets
β-cell
Primary animal islets / β-cells

Contributors to the T2DM hyperglycemea

Pancreas

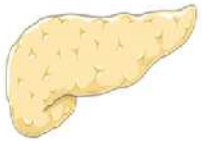

Islets of Langerhans:

β-cell ↘ insulin production

α-cell ↗ glucagon production

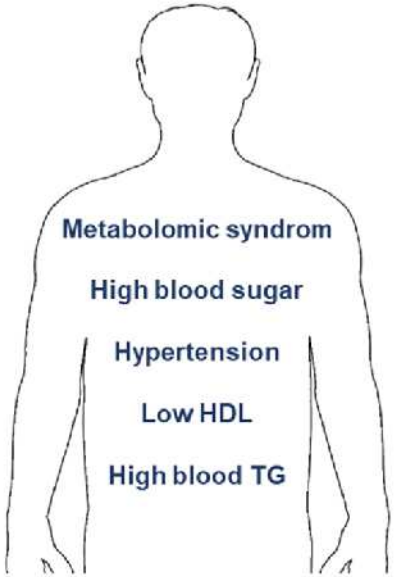

Muscle

Insulin resistance

Adipose tissue

Enhanced lipolysis

Small intestine

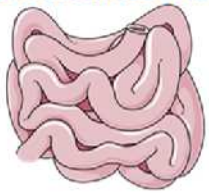

Deficiency of incretin effect

Liver

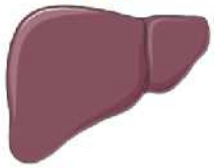

Insulin resistance

↗ glucose production

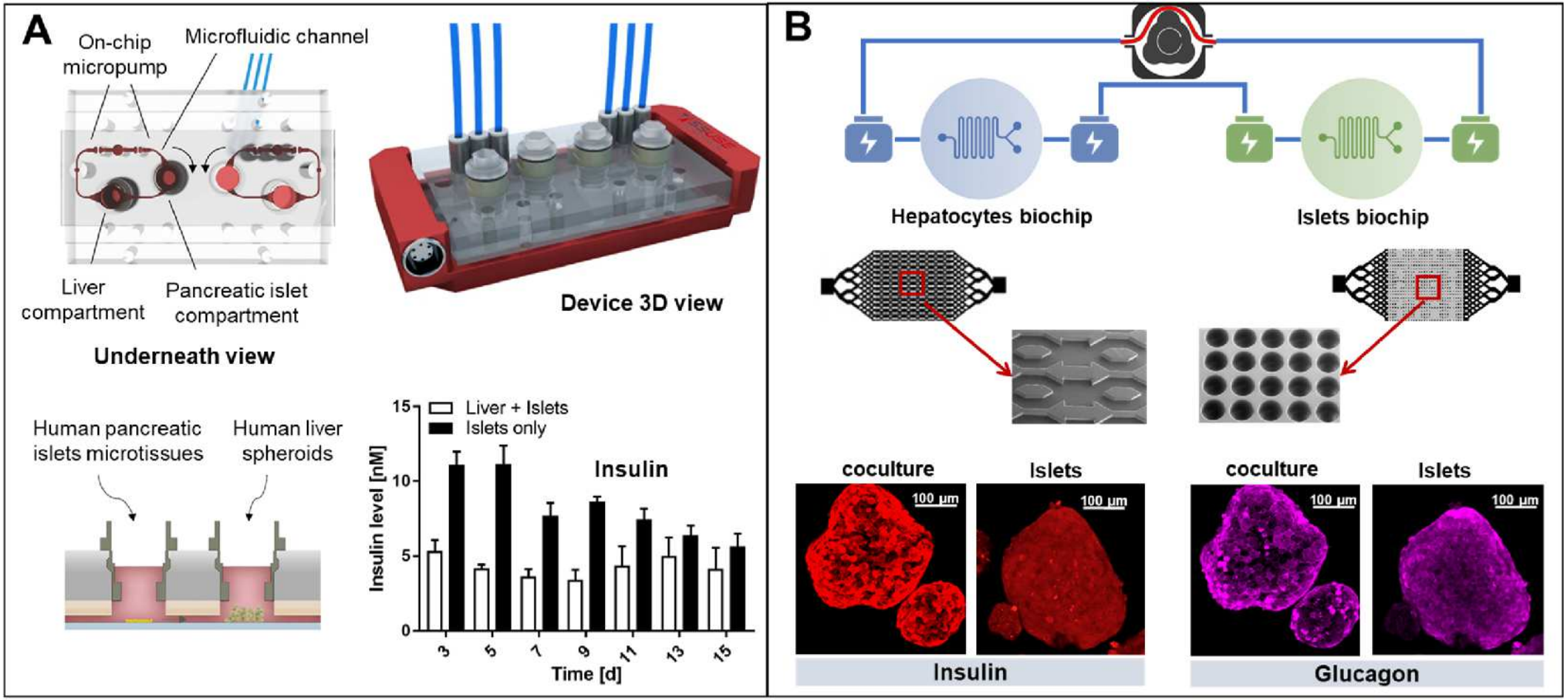
A
On-chip micropump
Microfluidic channel
Liver compartment
Pancreatic islet compartment
Underneath view
Device 3D view
Human pancreatic islets microtissues
Human liver spheroids
Liver + Islets
Islets only
Insulin
Insulin level [nM]
Time [d]
B
Hepatocytes biochip
Islets biochip
coculture
Islets
100 µm
Insulin
Glucagon